NASA/TM-2010-216183

Ares I-X Flight Test Vehicle: Stack 5 Modal Test

Ralph D. Buehrle, Justin D. Templeton, Mercedes C. Reaves, Lucas G. Horta, and James L. Gaspar
Langley Research Center, Hampton, Virginia

Paul A. Bartolotta
Glenn Research Center, Cleveland, Ohio

Russel A. Parks and Daniel R. Lazor
Marshall Space Flight Center, Huntsville, Alabama

January 2010

NASA STI Program . . . in Profile

Since its founding, NASA has been dedicated to the advancement of aeronautics and space science. The NASA scientific and technical information (STI) program plays a key part in helping NASA maintain this important role.

The NASA STI program operates under the auspices of the Agency Chief Information Officer. It collects, organizes, provides for archiving, and disseminates NASA's STI. The NASA STI program provides access to the NASA Aeronautics and Space Database and its public interface, the NASA Technical Report Server, thus providing one of the largest collections of aeronautical and space science STI in the world. Results are published in both non-NASA channels and by NASA in the NASA STI Report Series, which includes the following report types:

- TECHNICAL PUBLICATION. Reports of completed research or a major significant phase of research that present the results of NASA programs and include extensive data or theoretical analysis. Includes compilations of significant scientific and technical data and information deemed to be of continuing reference value. NASA counterpart of peer-reviewed formal professional papers, but having less stringent limitations on manuscript length and extent of graphic presentations.

- TECHNICAL MEMORANDUM. Scientific and technical findings that are preliminary or of specialized interest, e.g., quick release reports, working papers, and bibliographies that contain minimal annotation. Does not contain extensive analysis.

- CONTRACTOR REPORT. Scientific and technical findings by NASA-sponsored contractors and grantees.

- CONFERENCE PUBLICATION. Collected papers from scientific and technical conferences, symposia, seminars, or other meetings sponsored or co-sponsored by NASA.

- SPECIAL PUBLICATION. Scientific, technical, or historical information from NASA programs, projects, and missions, often concerned with subjects having substantial public interest.

- TECHNICAL TRANSLATION. English-language translations of foreign scientific and technical material pertinent to NASA's mission.

Specialized services also include creating custom thesauri, building customized databases, and organizing and publishing research results.

For more information about the NASA STI program, see the following:

- Access the NASA STI program home page at *http://www.sti.nasa.gov*

- E-mail your question via the Internet to help@sti.nasa.gov

- Fax your question to the NASA STI Help Desk at 443-757-5803

- Phone the NASA STI Help Desk at 443-757-5802

- Write to:
  NASA STI Help Desk
  NASA Center for AeroSpace Information
  7115 Standard Drive
  Hanover, MD 21076-1320

NASA/TM-2010-216183

Ares I-X Flight Test Vehicle: Stack 5 Modal Test

Ralph D. Buehrle, Justin D. Templeton, Mercedes C. Reaves, Lucas G. Horta, and James L. Gaspar
Langley Research Center, Hampton, Virginia

Paul A. Bartolotta
Glenn Research Center, Cleveland, Ohio

Russel A. Parks and Daniel R. Lazor
Marshall Space Flight Center, Huntsville, Alabama

National Aeronautics and
Space Administration

Langley Research Center
Hampton, Virginia 23681-2199

January 2010

Acknowledgments

Thanks go to Winifred Feldhaus of NASA Langley Research Center for her assistance with finite element model development. The test execution phase at Kennedy Space Center (KSC) could not have been done without the support of many individuals. Special thanks go to the KSC instrumentation team led by Frank Walker. Logistics and test hardware integration went smoothly due to the dedicated KSC crew that included Russ Brucker, Trip Healey, Stephanie Heffernan, Teresa Kinney, Todd Reeves, Kara Schmitt, Mark Tillett, and Jim Wiltse. Lastly, thanks to our independent verification team of Jeff Lollock, Ryan Tuttle, and Joshua Hwung from Aerospace Corporation.

Available from:

NASA Center for AeroSpace Information
7115 Standard Drive
Hanover, MD 21076-1320
443-757-5802

Table of Contents

Abstract

Ares I-X was the first flight test vehicle used in the development of NASA's Ares I crew launch vehicle. The Ares I-X used a 4-segment reusable solid rocket booster from the Space Shuttle heritage with mass simulators for the 5th segment, upper stage, crew module and launch abort system. Three modal tests were defined to verify the dynamic finite element model of the Ares I-X flight test vehicle. Test configurations included two partial stacks and the full Ares I-X flight test vehicle on the Mobile Launcher Platform. This report focuses on the first modal test that was performed on the top section of the vehicle referred to as Stack 5, which consisted of the spacecraft adapter, service module, crew module and launch abort system simulators. This report describes the test requirements, constraints, pre-test analysis, test operations and data analysis for the Ares I-X Stack 5 modal test.

1.0 Introduction

The 327 foot 1.8 million-pound Ares I-X launch vehicle [1] is shown in Figure 1. Ares I-X consists of a 4-segment reusable solid rocket motor from the Space Shuttle heritage with mass simulators for the 5th segment, upper stage, crew module (CM) and launch abort system (LAS). Ares I-X was successfully launched on October 28, 2009. This was the first flight test for NASA's Ares I crew launch vehicle. Flight test data will provide important information on ascent loads, vehicle control, separation, and first stage reentry dynamics.

As part of hardware verification for Ares I-X, a series of modal tests were designed to verify the dynamic finite element model (FEM) used in loads assessments and flight control evaluations. The first three free-free bending mode pairs were defined as the target modes for the modal test based on the flight control requirements. Since a test of the free-free vehicle configuration was not practical within the projects constraints, calibration of the FEM was done using modal test data for three configurations in the nominal KSC integration flow. The first of these modal tests was performed in May 2009 on the Stack 5 subassembly, which included the topmost hardware from the Spacecraft Adapter Simulator to the Launch Abort System Simulator as shown in Figure 2. The second test was performed in July 2009 on the Stack 1 hardware, which included the center section from the 5th Segment Simulator through the Interstage. Finally, the fully integrated Ares I-X flight test vehicle (FTV) mounted to the Mobile Launcher Platform (MLP) was tested in August 2009 [2].

This report focuses on the Stack 5 modal test. The requirements are derived from the free-free bending target modes. Based on these requirements, FEM pre-test analysis is used to define the response transducer and shaker locations. Project constraints on instrumentation numbers and vehicle accessibility are also discussed as part of the transducer/shaker placement studies. Schedule constraints required that the team conduct the tests and verify the sufficiency of the data in a short four-day test period. Details of the modal test planning, setup, operation, and results are described. Comparisons between pre-test predictions and test data are also summarized.

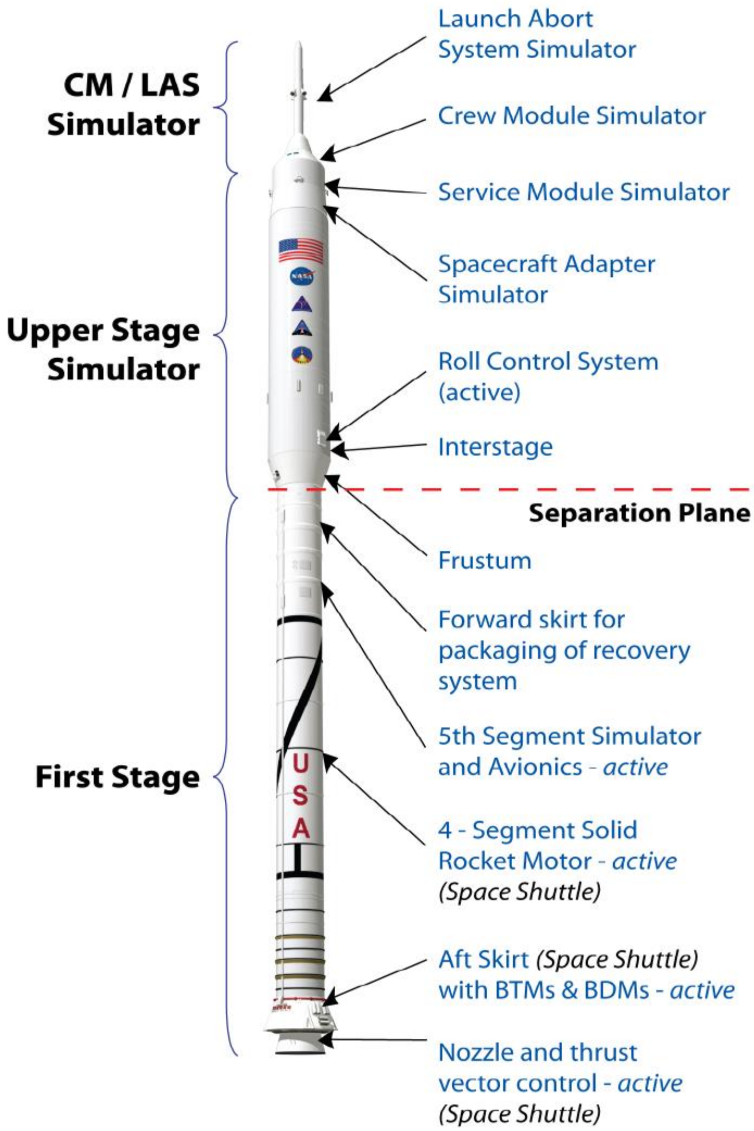

Figure 1 Ares I-X Flight Test Vehicle [1]

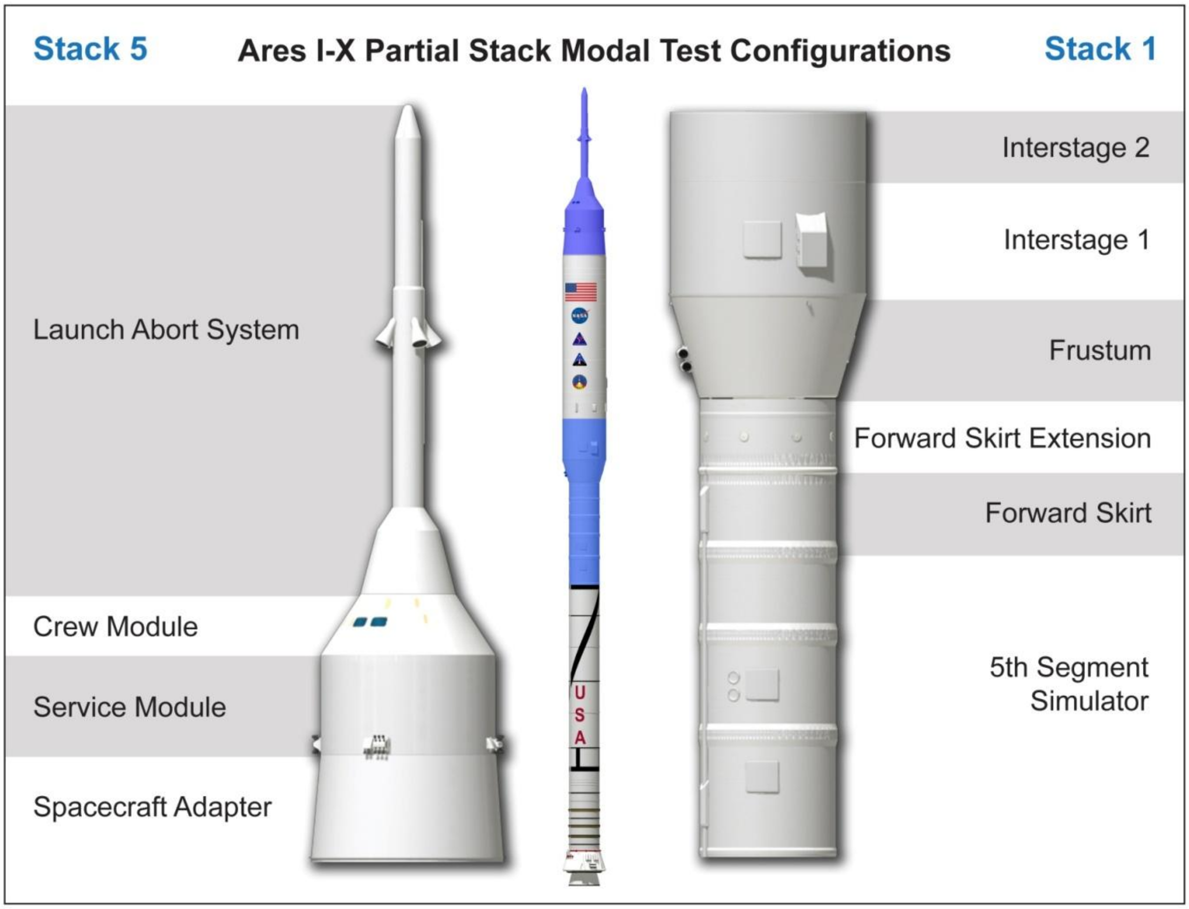

Figure 2 Ares I-X Subassembly Modal Test Configurations

2.0 Pre-Test Planning

2.1 Test Requirements

The Stack 5 modal test was meant to provide an early assessment of FEM adequacy for the subassembly. The project emphasized minimal instrumentation to characterize the bending modes and did not provide hard limits on test/analysis orthogonality metrics. Initially, the goal prior to conducting the pre-test analysis was for approximately 20 sensor locations with biaxial accelerometers for capturing the bending modes. To minimize impact to the program schedule and cost, test durations and configurations were restricted to what was available during the normal vehicle integration flow. Because no special provisions were made for testing, the stack 5 subassembly was tested while shimmed to the floor in High Bay 4 of the Vehicle Assembly Building (VAB). Testing on the floor of the VAB added two significant constraints to the test setup. First, shaker mounting was restricted to locations accessible from an external lift. Second, the boundary condition was unknown and would need to be compensated for in the analysis. Early in the planning stage the test team recognized the risk associated with unknown boundaries and proceeded with an effort to correct for boundary interface compliance [3], and planned for additional measurements across the boundaries. The boundary condition will be further described in the Test Description section.

For flight control, the first three free-free bending mode pairs of the flight test vehicle were critical. Based on these modes, a traceability study [4] was used to define the target modes for the subassembly tests. For the Stack 5 configuration, the first bending mode pair was defined as the target mode set due to their importance for describing the 3rd bending mode pair for the integrated flight test vehicle.

2.3 Pre-Test Analysis

The Stack 5 configuration (see Figure 3) consisted of the spacecraft adapter (SA), service module (SM), crew module (CM) and launch abort system (LAS) mounted on the super-segment assembly stand (SSAS) and heavy weight upper stage simulator (USS) transportation cart. The cart had the wheels removed and was shimmed level on the floor of the VAB High Bay 4. Although the SSAS and heavy weight cart were not part of the flight vehicle, models of these segments were added to the FEM to represent the tested configuration. A nominal boundary spring stiffness of $6X10^7$ lb/in was used at the shim locations to account for the boundary compliance in the pre-test analysis. FEM predictions of the first six modes are shown in Table 1 with the target modes highlighted. The corresponding mode shapes for the X-Z plane are shown in Figure 4. During pre-test analysis, it was observed that the system bending modes (modes 3 and 4) were sensitive to the selected boundary stiffness but the LAS bending modes were relatively insensitive.

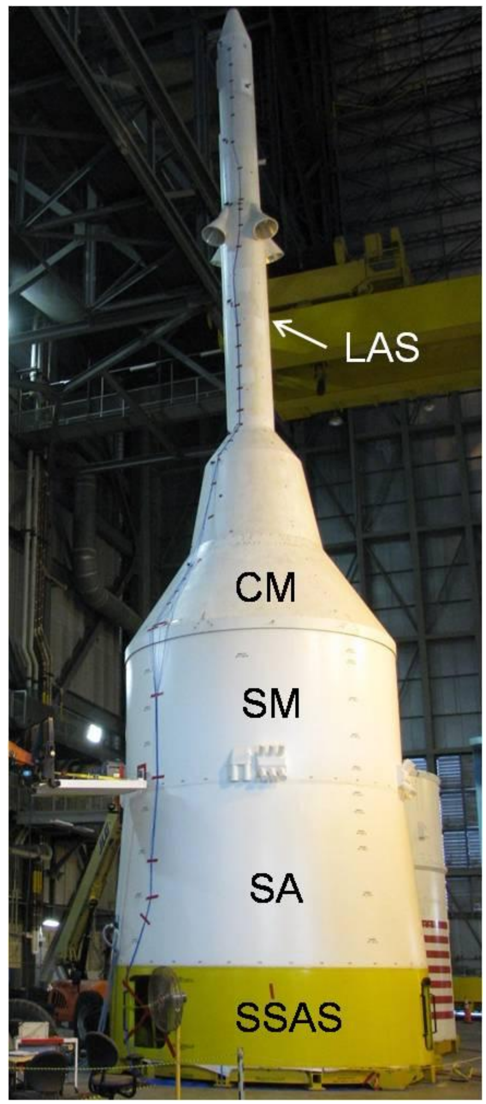

Figure 3 Stack 5 test configuration

Based on the first six bending modes, sensor and shaker placement was performed using the effective independence [5] technique along with engineering judgment. The resulting measurement locations included 20 biaxial and 10 triaxial sets of transducers as shown in Figure 5. The 45,042 degree of freedom (DOF) FEM was reduced to a 70 DOF test model. The corresponding cross-orthogonality between the reduced model (corresponding to the test instrumentation set) and the full model is used to assess the adequacy of the test instrumentation set as shown in Figure 6. Diagonal terms for the cross-orthogonality matrix are $\geq$0.95 and the off-diagonal terms are generally <0.1. However, the off-diagonal terms for mode pair 5, 6 were 0.3. This was deemed acceptable for this minimal instrumentation set. Figure 5 also shows the two shaker locations that were determined to be optimal within the elevation constraints. The elevation constraint was due to the test hardware resting on the floor of the VAB without surrounding infrastructure, which required heavy lift equipment for shaker positioning.

Table 1 Pre-Test Analysis Modes for Stack 5

Mode No.	Frequency (Hz)	Mode Description
1	4.60	LAS 1st Bending Mode (X-Z Plane)
2	4.67	LAS 1st Bending Mode (X-Y Plane)
3	12.2	System Bending (X-Z Plane)
4	14.7	System Bending (X-Y Plane)
5	26.1	LAS 2nd Bending Mode (X-Z Plane)
6	26.2	LAS 2nd Bending Mode (X-Y Plane)

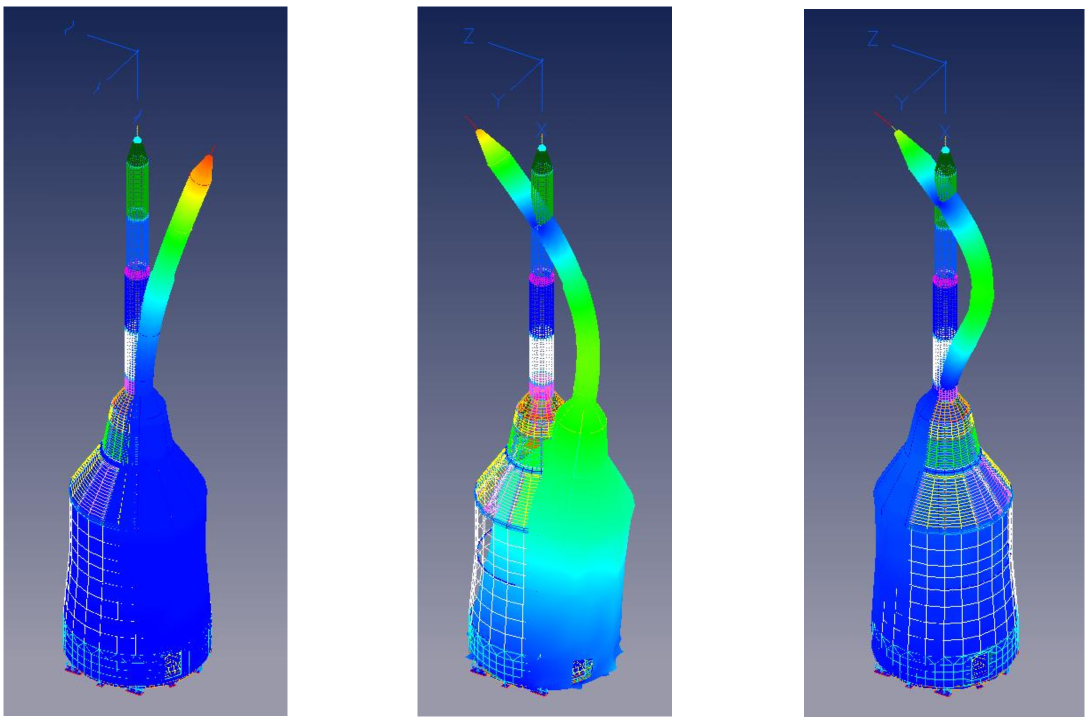

4.60 Hz, 4.67 Hz
Mode 1 X-Z
Mode 2 X-Y

12.2 Hz, 14.7 Hz
Mode 3 X-Z
Mode 4 X-Y

26.1 Hz, 26.2 Hz
Mode 5 X-Z
Mode 6 X-Y

Figure 4 FEM Pre-Test Analysis Mode Shapes for Stack 5

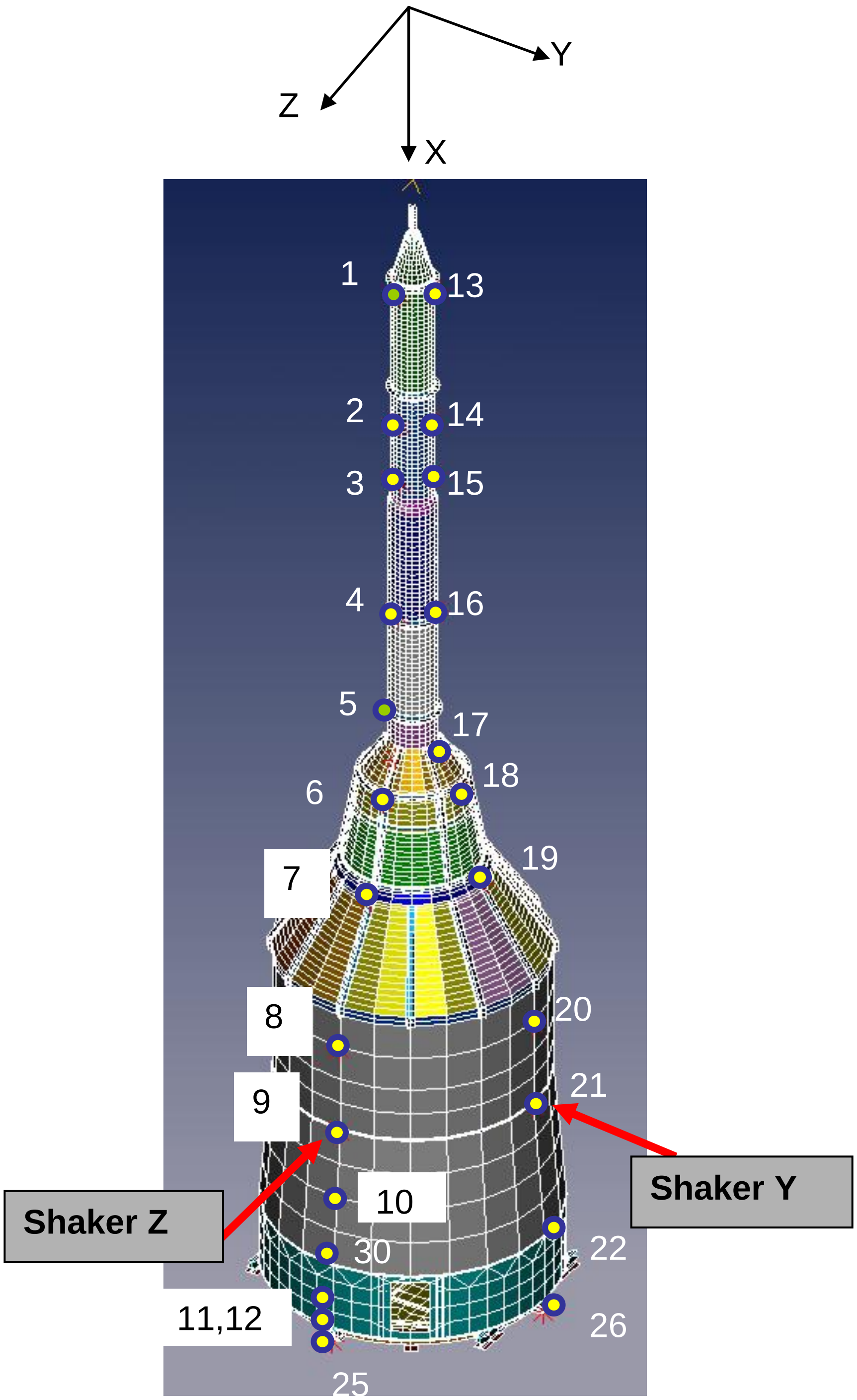

Figure 5 Stack 5 sensor/shaker locations

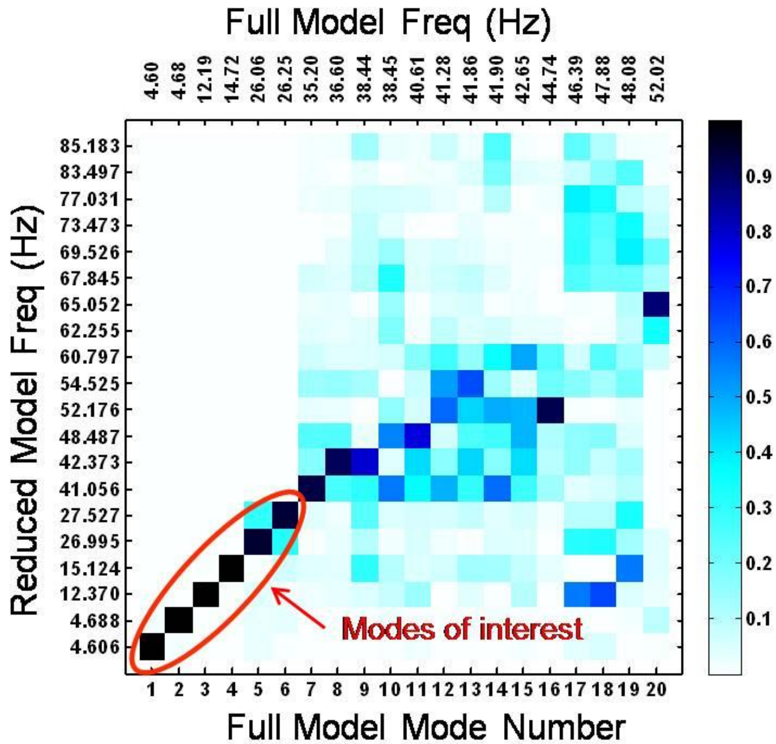

Figure 6 Stack 5 cross-orthogonality

3.0 Test Description

3.1 Test Article

Testing of the Stack 5 configuration was performed in High Bay 4 of the VAB as shown in Figure 7. The Stack 5 hardware was mounted on the SSAS and heavy weight transportation cart, which was shimmed to the VAB floor at twelve locations (See Figures 8 and 9). A gap check was performed by sliding a piece of paper along the shim. It was found that the shim locations at approximately 25, 110, 175, 200, and 275 degrees had only partial contact. Shim locations at 0 and 50 degrees were not measured due to access limitations.

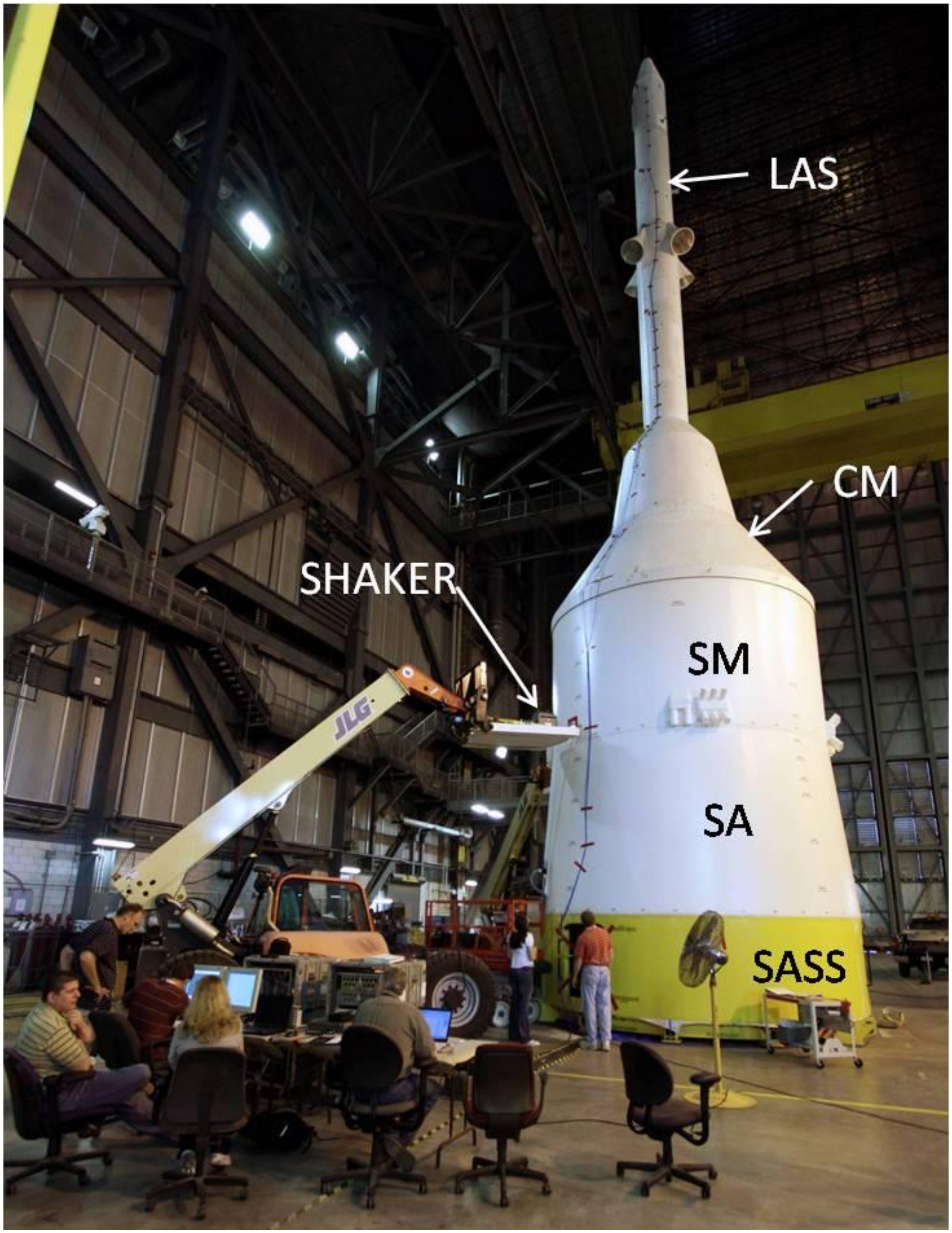

Figure 7 Stack 5 modal test setup

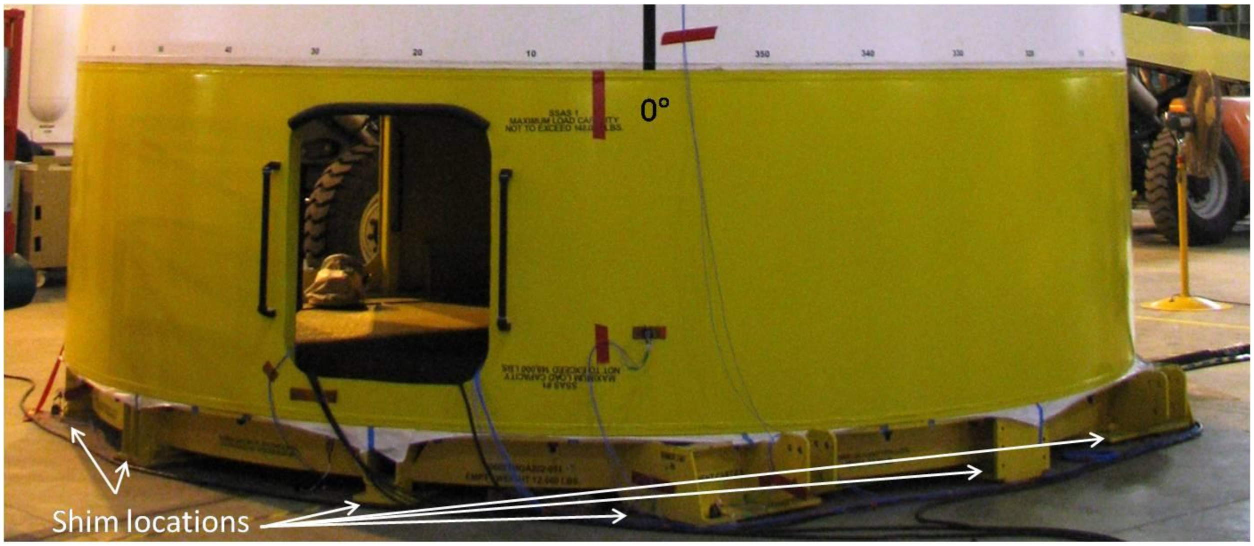

Figure 8 Shim locations around 0-degree side of Stack 5

Figure 9 Shim location and ground accelerometers at 90° orientation

3.2 Test Instrumentation

Accelerometer and shaker locations for the Stack 5 configuration are shown in Figure 5. The as-installed locations and orientations are listed in Table 2 using the Flight Test Vehicle (FTV) Structural Body Coordinate System as a reference. Accelerometer installation was performed according to KSC Work Plan FA-GIE-0030, Ares-IX Stack 5 Modal Test-Ground Instrumentation Support. Representative photographs of the accelerometer installations are provided in Figures 10 and 11. In general, capacitive accelerometers (PCB Model 3701GFA3G and 3701M 15) were used to measure the dynamic response of the test article. In addition to the capacitive accelerometers, two general-purpose triaxial accelerometers were mounted on each of the shakers (locations 33, 34) in case there was coupling of the test article and the shaker telehandler supports (see section 2.3).

Table 2 As-installed Accelerometer Locations

Location Number	X-station (inches)	Angle (degrees)	Description	Measurement Axis
1	199.0	180.0	*LAS pre-installed	-Y, Z
2	313.9	0.0	LAS	Y, Z
3	382.6	0.0	LAS	Y, Z
4	480.5	0.0	LAS	Y, Z
5	565.2	180.0	*LAS pre-installed	-Y, Z
6	631.6	0.0	LAS	Y, Z
7	708.7	0.0	LAS/CM	Y, Z
8	816.0	0.0	*SM	Y, -Z
9	880.5	0.0	*SM; Shaker 1 (-Z)	Y, -Z
10	943.0	0.0	*SA	Y, -Z
11	1041.0	0.0	SASS	-X, Y, Z
12	1068.3	0.0	Cart side opposite 25	-X, Y, Z
13	199.8	270.0	LAS	Y, Z
14	313.9	270.0	LAS	Y, Z
15	382.6	270.0	LAS	Y, Z
16	480.5	270.0	LAS	Y, Z
17	602.	270.0	LAS	Y, Z
18	631.6	270.0	LAS	Y, Z
19	708.7	270.0	LAS/CM	Y, Z
20	816.1	270.0	*SM	-Y, Z
21	880.0	270.0	*SM; Shaker 2 (-Y)	-Y, Z
22	995.0	270.0	*SA in-line with 26	-X, -Y, Z
23	995.0	90.0	*SA in-line with 27	-X, Y, Z
24	995.0	180.0	*SA in-line with 28	-X, Y, Z
25	1069.5	0.0	Ground side opposite 12	-X, Y, Z
26	1069.5	267.0	Ground in-line with 22	-X, Y, Z
27	1069.5	85.0	Ground in-line with 23	-X, Y, Z
28	1069.5	180.0	Ground in-line with 24	-X, Y, Z
29	400.2	180.0	*LAS pre-installed	-Y, Z
30	995.0	0.0	* SA in-line with 25	-X, Y, -Z
31	874.0	5.0	Shaker 1 Impedance	-Z
32	874.0	275.0	Shaker 2 Impedance	-Y
33	-	-	On shaker 1	X, Y, Z
34	-	-	On shaker 2	X, Y, Z

*Accelerometers mounted internally

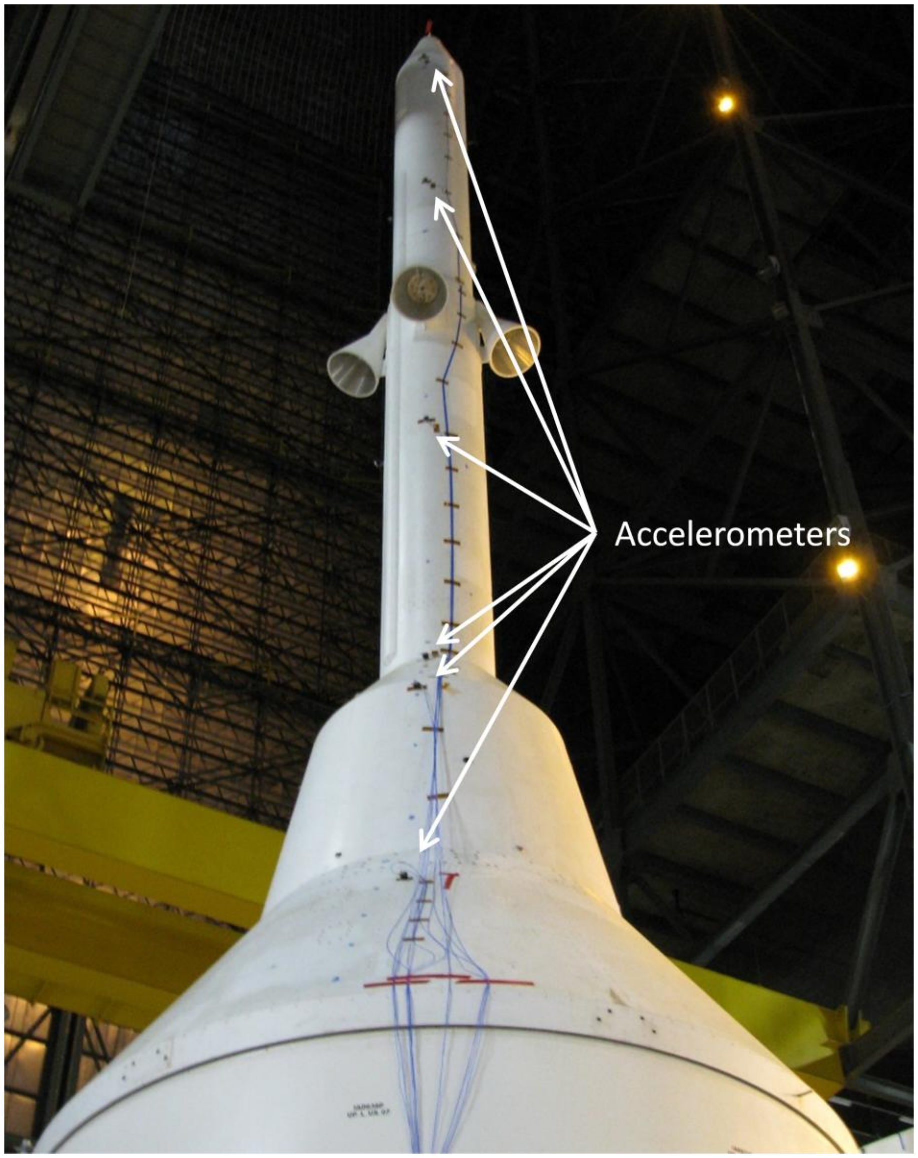

Figure 10 External accelerometers at 270-degree orientation

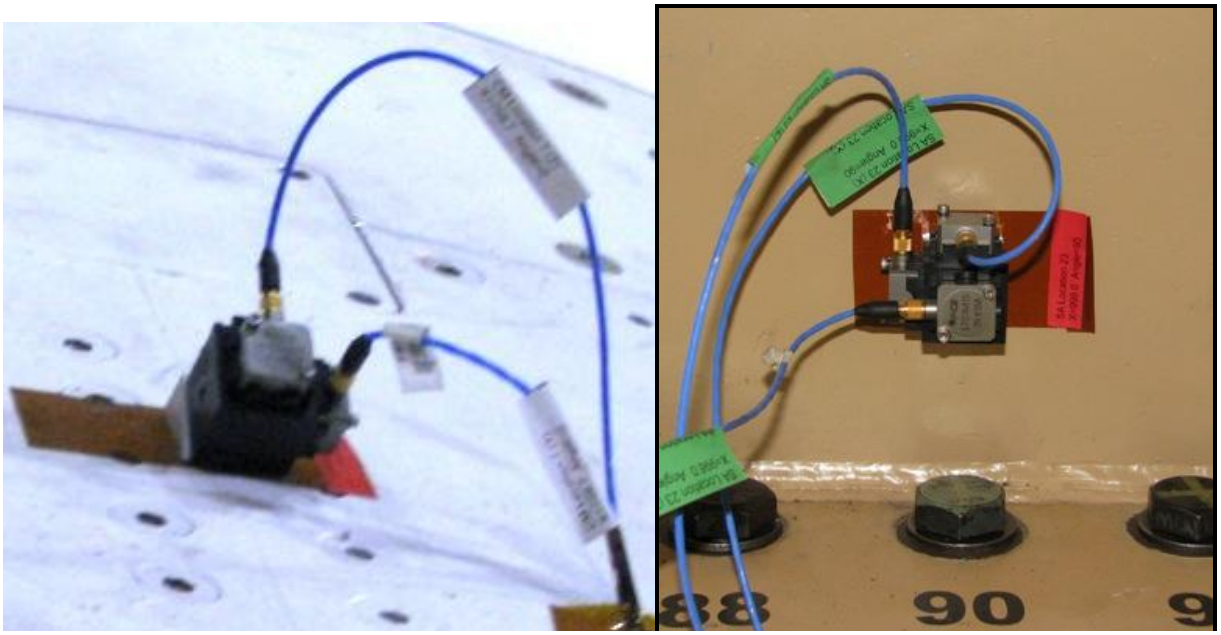

Figure 11 External biaxial accelerometer configuration (left) and internal triaxial mounting configuration (right)

3.3 Excitation Systems

Two MB Dynamics Model 250 electro-dynamic shakers were used to provide excitation to Stack 5 as shown in Figure 12. The shakers were installed on telehandlers during testing. The telehandler lifting cylinder was locked out (see Figure 13) and the wheels were chocked during testing. Figure 14 shows shaker 2 being aligned for installation at the 275° orientation. The shakers were attached to the test article through a ¼-28 threaded rod stinger designed to impart axial loads while minimizing any lateral excitation. The stinger was attached to the test article through an impedance sensor and adapter plate. These adapter plates were attached to the test article with dental cement. The adapter plates had threaded holes in them to which the impedance head was attached. The adapter plates were centered 12” above the SA/SM interface.

The shakers were operated simultaneously for Multiple Input Multiple Output (MIMO) burst random testing. Several sine sweeps using a single shaker were also performed. The idle shaker was disconnected from the test article during the sine sweeps. In addition to the shaker test, impact tests were performed for four excitation positions with all response data recorded simultaneously. A PCB Piezotronics Model 086B20 hammer was used for impact testing as shown in Figure 15.

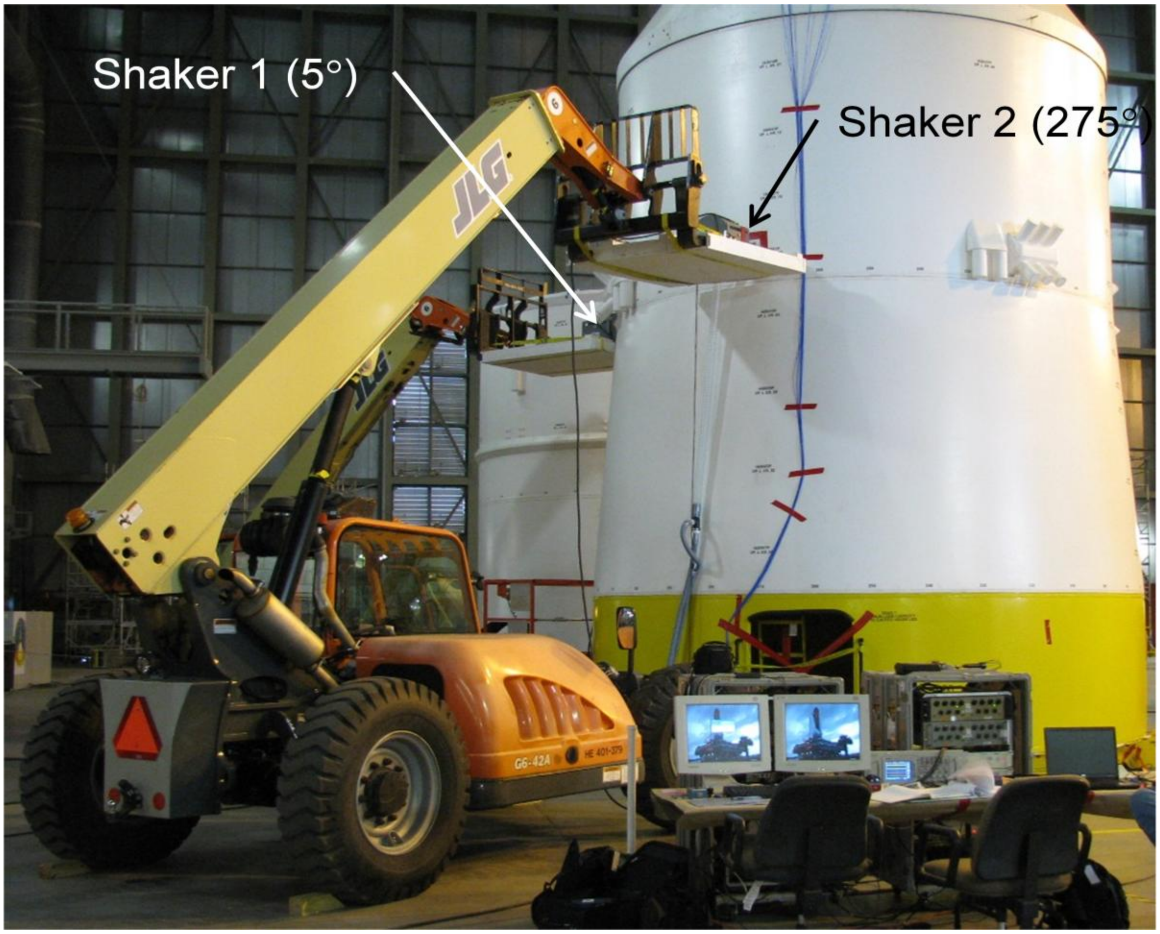

Figure 12 Shakers setup on telehandlers

Figure 13 Installation of lockout hardware for telehandler lift

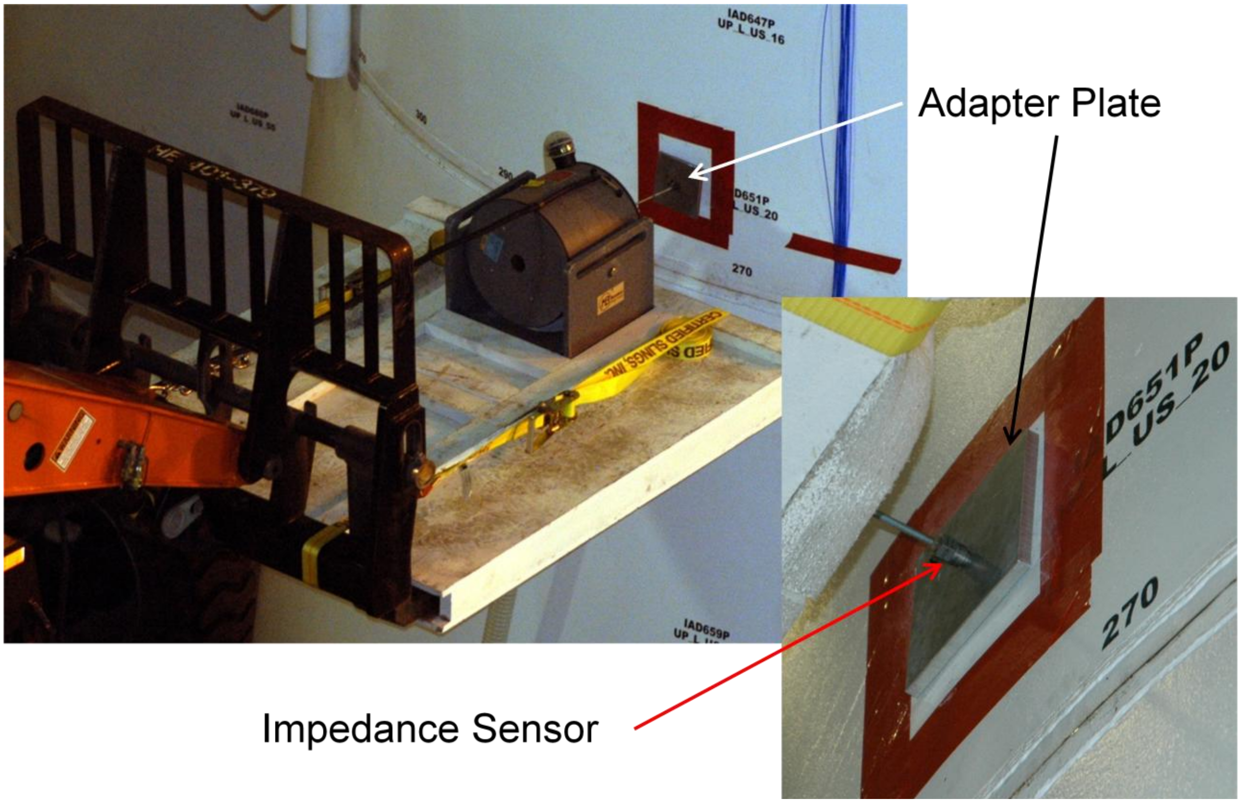

Figure 1 Shaker 2 being aligned for attachment to test article

Figure 15 Impact hammer excitation at location 21

3.4 Data Acquisition System

The 96-channel data acquisition system (DAS) consisted of six 16 channel 24-bit VXI data acquisition cards in a single 13-slot VXI mainframe chassis. Sufficient channels were available to simultaneously sample and record all data. A 16-bit VXI source card in the same chassis provided separate source signals for the excitation system. A Firewire interface card allowed the DAS to be controlled by a data acquisition computer running m+p International's Smart Office Analyzer software. During the test, the software calculated the FRFs from the acceleration and force measurements. For all shaker tests, time and FRF data was stored directly to the computer's hard drive as it was acquired. For impact testing, only the FRF's were stored. After each test, the FRFs were exported to a universal file format and supplied to the test team for on-site modal parameter estimation. For a complete list of the equipment, see Appendix B.

A picture of the signal conditioner rack and data acquisition rack as they were configured for the modal test is shown in Figure 16. The signal conditioner rack is located on the left side of the figure, and the data acquisition rack is located on the right. The signal conditioner rack contained four filters (top of rack, two per box). The top two filters were used to filter the source signals before they reached the excitation system. The signal conditioner rack also contained five of the six signal conditioners used during the test. All of these signal conditioners, plus the filters and the VXI chassis were powered by an Uninterruptible Power Supply (UPS) in the bottom of the signal conditioner rack. The other signal conditioner was located inside the test article to facilitate cable routing and was powered by an extension cord from another power source. A separate UPS located in the bottom of the data acquisition rack was used to power the computer. This isolated the typically noisy computer power supply from the rest of the DAS equipment.

The majority of the signal conditioner channels were routed directly to the data acquisition cards in the VXI chassis using custom-built cables (dark gray cables). The rest of the channels were connected by BNC cables to patch panels at the top of the data acquisition rack. These patch panels were then connected to the data acquisition cards at the bottom of the rack. For more information on the connections from the instrumentation to the data acquisition system, see the channel mapping in Appendix C.

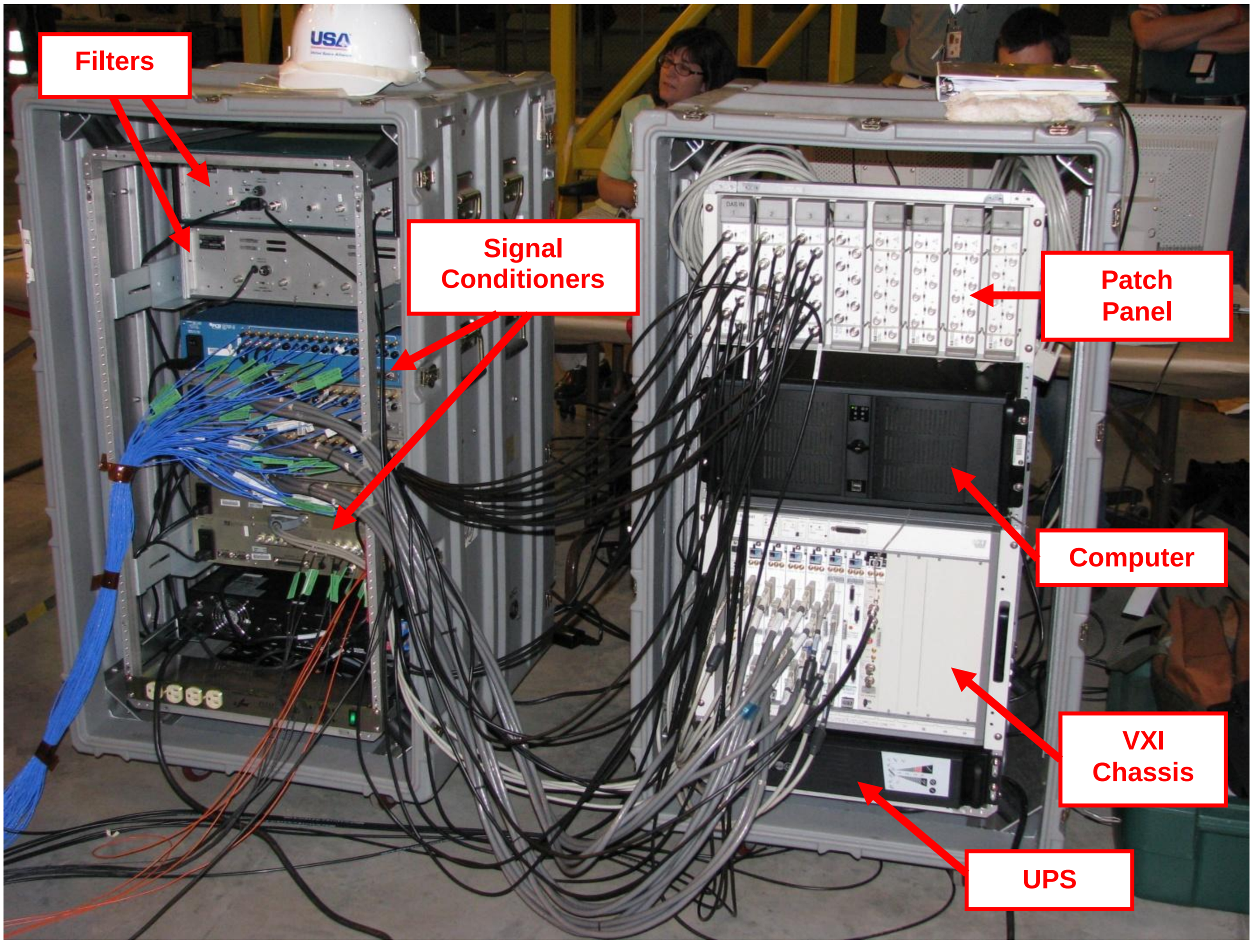

Figure 16. Data acquisition system configuration

4.0 Stack 5 Test Operation and Data Analysis

4.1 Summary of Tests

The modal test was performed by applying a measured excitation force to the test article and measuring the acceleration response at selected locations. The FRFs were calculated as the ratio of the acceleration response to the input force. Modal parameters (natural frequencies, damping factors, and mode shapes) were then estimated from the FRFs. Both the measured FRF data and modal parameter estimates were compared with the pre-test predictions to ensure that sufficient data was acquired to capture the target modes of interest. The primary datasets for modal parameter estimation were FRFs for multi-input random excitation at several force levels. Sine sweeps using a single shaker were used to check for linearity of selected modes with respect to force level. In addition, impact testing on the LAS was used to provide additional data for model verification.

The test data that was acquired during the Stack 5 modal test is listed in table 3. Ambient noise and impact datasets were acquired during pre-test activities on May 26th and 27th, 2009, listed as tests SS5-1 through SS5-4. All other datasets were acquired on May 29th, 2009. Testing on the

May 29th began with a series of burst random tests that varied burst percentage, number of averages, and force level. Following the burst random tests, one ambient noise measurement was made. Finally, force-controlled sine sweeps were performed at different force levels and sweep rates to investigate nonlinearities for modes 2 through 4. Sweeps were not performed on mode 1 due to limited test time.

Table 3 Super Stack 5 Modal Test Datasets

Test	Run	Type	Level	Direction(s)	Range
SS5-1	n/a	Ambient Noise	n/a	n/a	0 to 50 Hz
SS5-3	n/a	Impact	100 lb-pk	16Y-	0 to 50 Hz
				4Z-	
				9Z-	
SS5-4	n/a	Impact	100 lb-pk	21Y-	0 to 50 Hz
SS5-2	n/a	Ambient Noise	n/a	n/a	0 to 50 Hz
SS5-5	n/a	Burst Random (75%, 20 avg)	8 lb-rms	9Z-, 21Y-	1 to 50 Hz
SS5-6	n/a	Burst Random (50%, 20 avg)	20 lb-rms	9Z-, 21Y-	1 to 50 Hz
SS5-7	n/a	Burst Random (50%, 40 avg)	20 lb-rms	9Z-, 21Y-	1 to 50 Hz
SS5-8	n/a	Burst Random (50%, 20 avg)	50 lb-rms	9Z-, 21Y-	1 to 50 Hz
SS5-9	n/a	Burst Random (50%, 20 avg)	90 lb-rms	9Z-, 21Y-	1 to 50 Hz
SS5-10	n/a	Ambient Noise	n/a	n/a	0 to 50 Hz
SS5-11	1	Sine Sweep (1.0 Hz/min)	10 lb-pk	21Y-	3.75 to 4.84 Hz
	2	Sine Sweep (0.5 Hz/min)	20 lb-pk		
	3	Sine Sweep (0.25 Hz/min)	20 lb-pk		
	4	Sine Sweep (0.1 Hz/min)	20 lb-pk		4.05 to 4.54 Hz
	5	Sine Sweep (0.1 Hz/min)	50 lb-pk		
	6	Sine Sweep (0.1 Hz/min)	100 lb-pk		
SS5-12	1	Sine Sweep (0.2 Hz/min)	20 lb-pk	21Y-	9.22 to 10.32 Hz
	2	Sine Sweep (0.2 Hz/min)	100 lb-pk		
SS5-13	1	Sine Sweep (0.2 Hz/min)	20 lb-pk	9Z-	8.34 to 9.31 Hz
	2	Sine Sweep (0.2 Hz/min)	100 lb-pk		

4.2 Impact Data Analysis

Prior to connecting the shakers, impact tests were performed to get an initial assessment of the modal properties. Sampling parameters were a 1024 Hz sample rate, 8-second block size, and 5 averages. Figures 17 and 18 show results for impacts on the LAS. The target bending modes were identified but the frequencies for the system bending modes (modes 3 and 4 from Table 1) were well below the pre-test predictions. These differences were attributed to the unknown boundary stiffness.

4.3 Burst Random Data Analysis

The burst random excitation data sets were the primary data for mode shape estimation and model calibration. In this section, the data quality from these tests is evaluated based on the FRF, coherence, reciprocity, and input force characteristics. Measurement linearity with force amplitude is also examined for the three random input test levels. A comparison of the burst random and impact data is also used to verify data consistency.

Selection of the resolution for the burst random datasets was a function of both the desired data quality and the limited test time available [6]. The data was sampled at 128 Hz with a block size of 32 seconds to achieve the desired resolution of 0.03125 Hz. Several data sets were acquired to examine the burst percentage and number of averages. Based on this data, a 50% burst with 20 averages was used to acquire burst random data at three force levels.

Sample FRF and coherence data from the 90 lb-rms burst random test is shown in figures 19 and 20 below. The blue curves show the drive point FRFs, and the green curves show the FRFs for the topmost locations. The red and teal curves show the multiple coherence between these response locations and both input forces. The measurements shown had good coherence values (> 0.8) in the vicinity of all target modes. From the figures, it is apparent that the first two modes in the Z-direction and first mode in the Y-direction were well defined, whereas the modes above 20.0 Hz were closely spaced but distinguishable. The second mode in the Y-direction does not have a clean peak, but is instead flattened at the top. This flattening at the peak is possibly due to nonlinearities in the boundary associated with the gaps observed for some of the shims at the cart to floor interface, and/or noise that was present in every test at harmonics of 10.0 Hz. The 10 Hz noise that was present during testing is illustrated in figure 21, which shows the autopower measurement of a ground accelerometer during the ambient noise test, SS5-10.

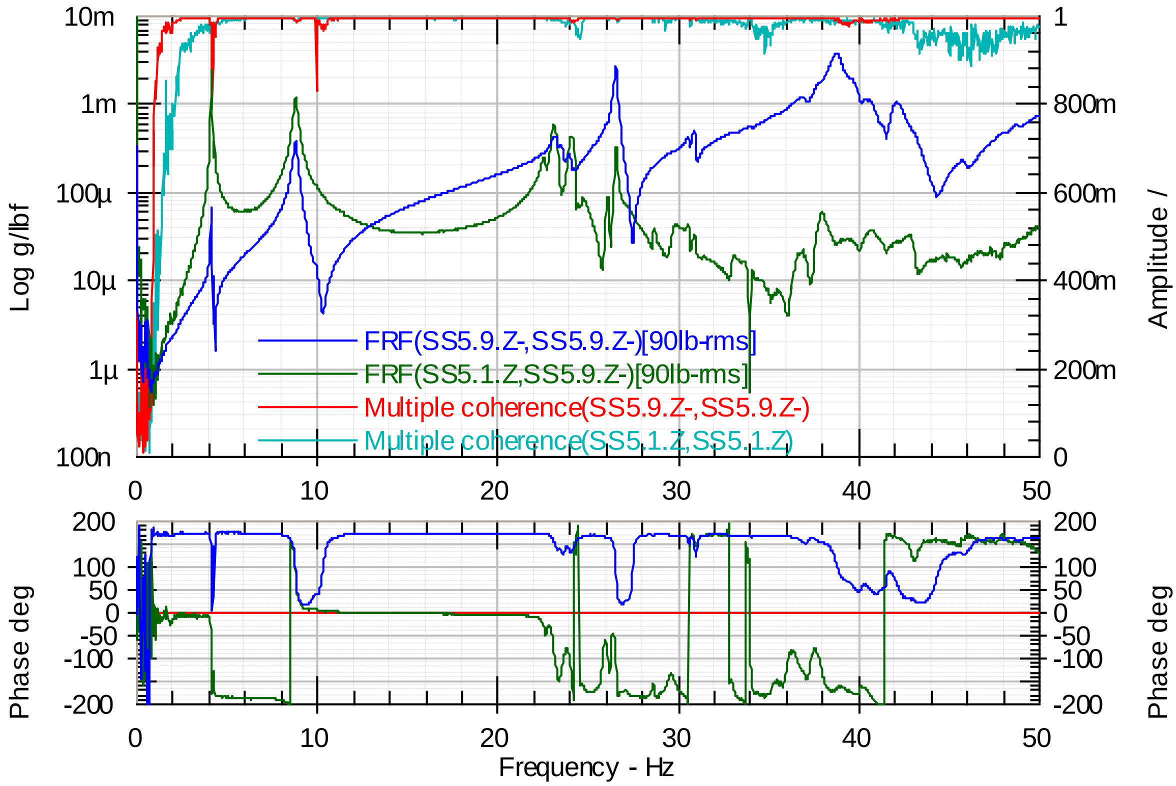

Figure 19 Z-direction FRFs from 90 lb-rms burst random test

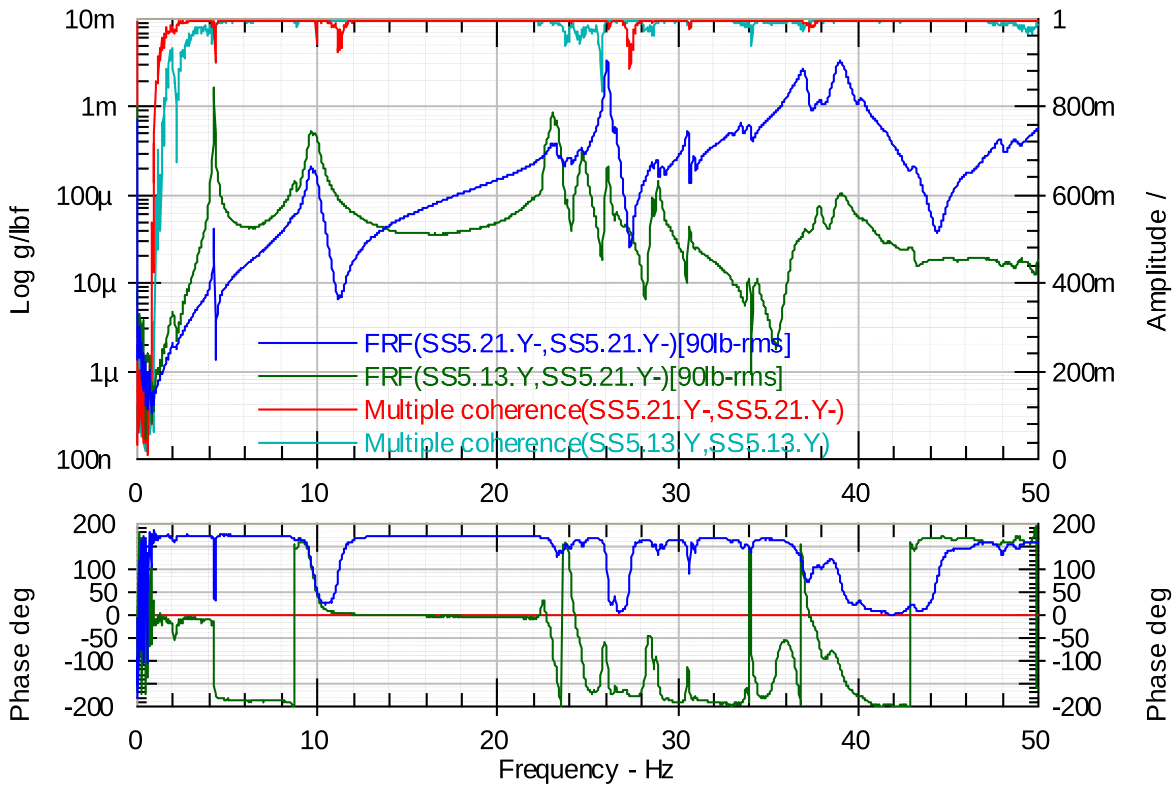

Figure 20 Y-direction FRFs from 90 lb-rms burst random test

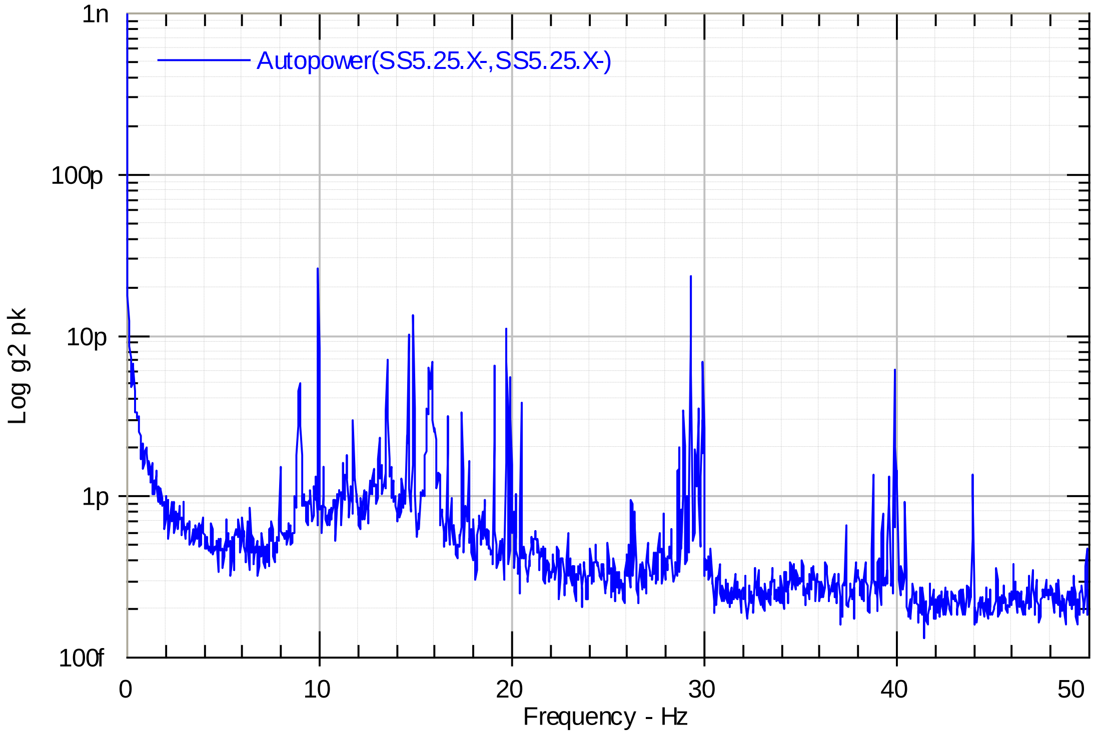

Figure 21 Autopower of ground accelerometer during ambient noise test SS5-10

The result of a reciprocity check from the 90 lb-rms burst random test is shown in figure 22, which compares the impedance head accelerometer FRFs. Channel 32Y is the impedance head accelerometer for the shaker at 21Y- and channel 31Z is the impedance head accelerometer for the shaker at 9Z-. As shown, the structure exhibited good reciprocity for the Multi-Input Multi-Output (MIMO) burst random test.

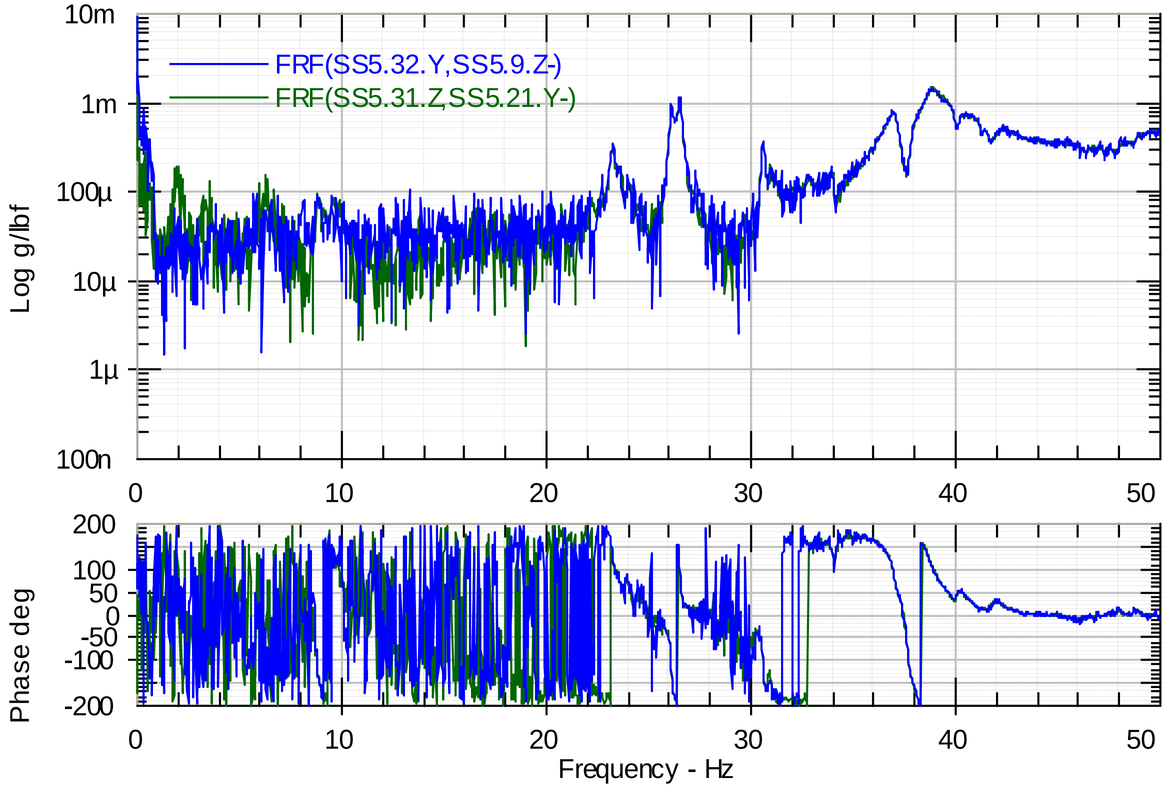

Figure 22 Reciprocity from 90 lb-rms burst random test with impedance head accelerometers

Prior to testing, there was concern that the telehandlers supporting the shakers may adversely affect the shaker input characteristics. Figure 23 shows the force spectra measured during the 90 lb-rms burst random test. The force input spectrum shows good input across the bandwidth as indicated by the relatively flat response with no significant dips.

Another check on the input forces was done using principal component analysis. Results are shown for the 90 lb-rms burst random test in figure 24. The separation between the principal components was no greater than 5 dB, indicating that there was little to no correlation between the input force signals in the bandwidth of interest. This conclusion can also be reached by observing the coherence between the input forces, which was much less than 1 across the frequency band.

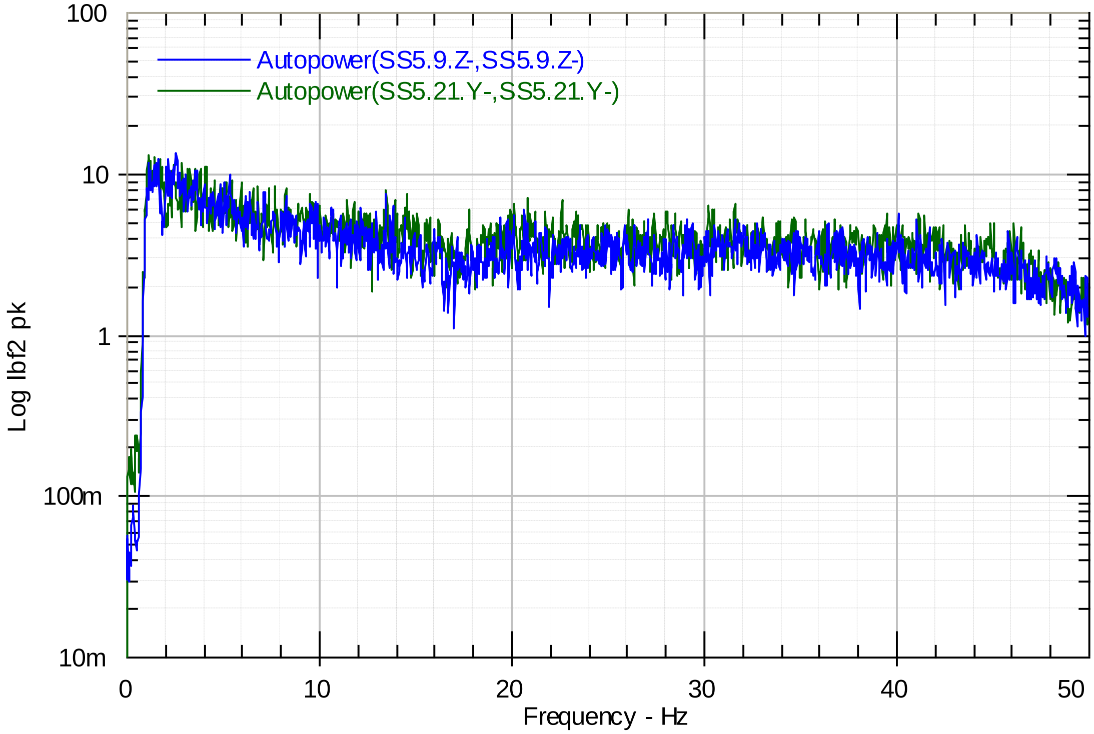

Figure 23 Input autopower from 90 lb-rms burst random test

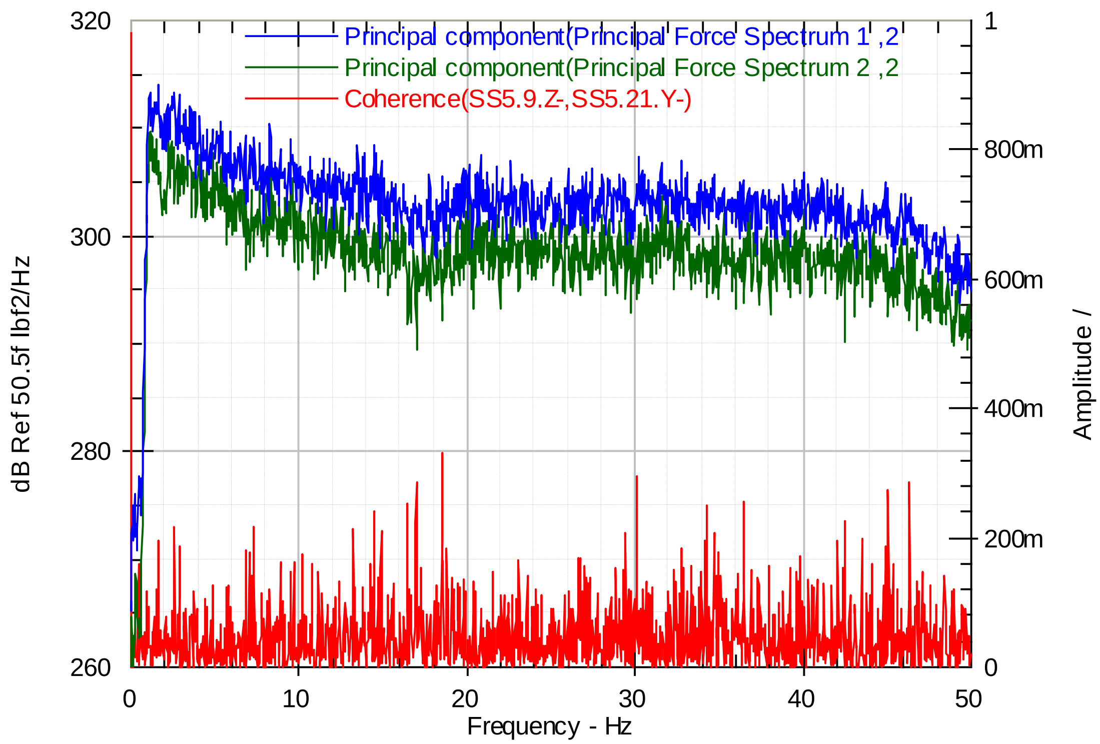

Figure 24 Principal input spectra and coherence from 90 lb-rms burst random test

Figures 25 and 26 show a comparison of the burst random FRFs for three force levels. As shown, the Stack 5 subassembly responded linearly, with peak frequency changes less than or equal to 1.06% between the 20 and 90 lb-rms burst random tests. Because the nature of random excitation is to linearize test results, sine sweep tests were also performed to investigate possible nonlinearities in the structure.

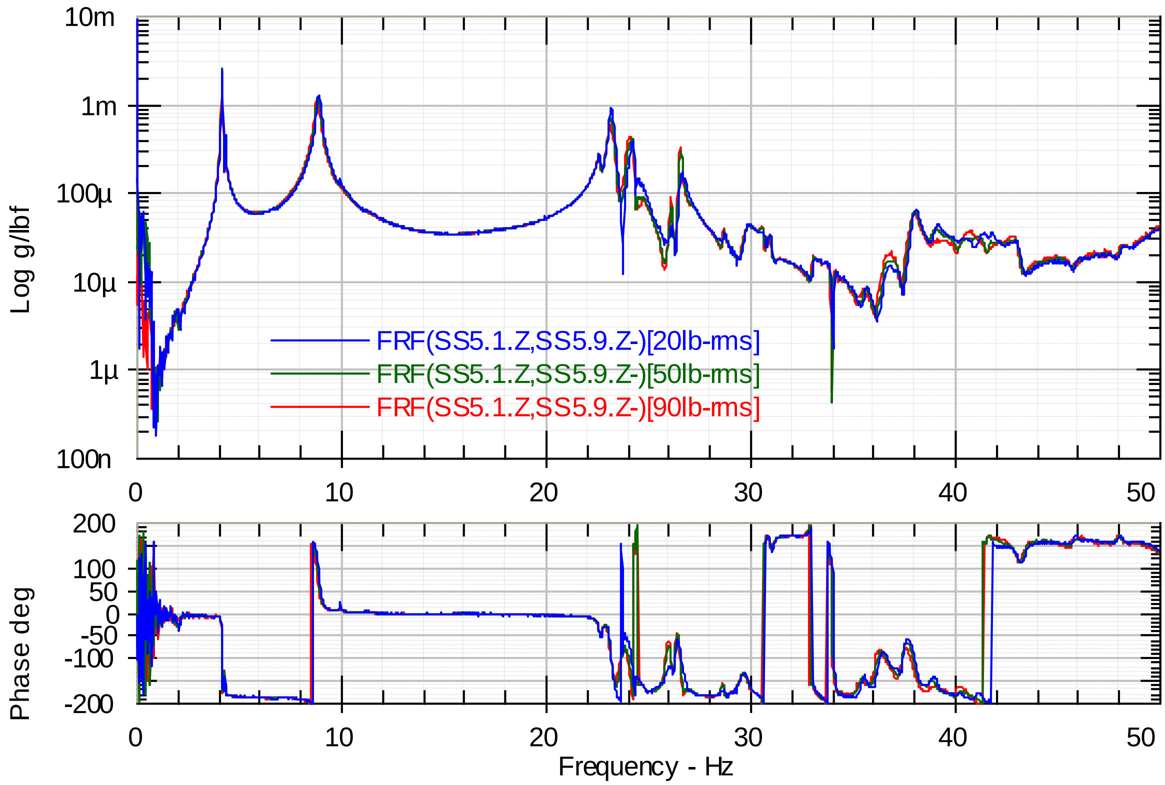

Figure 25 Z-direction FRFs from burst random tests SS5-6, SS5-8, and SS5-9

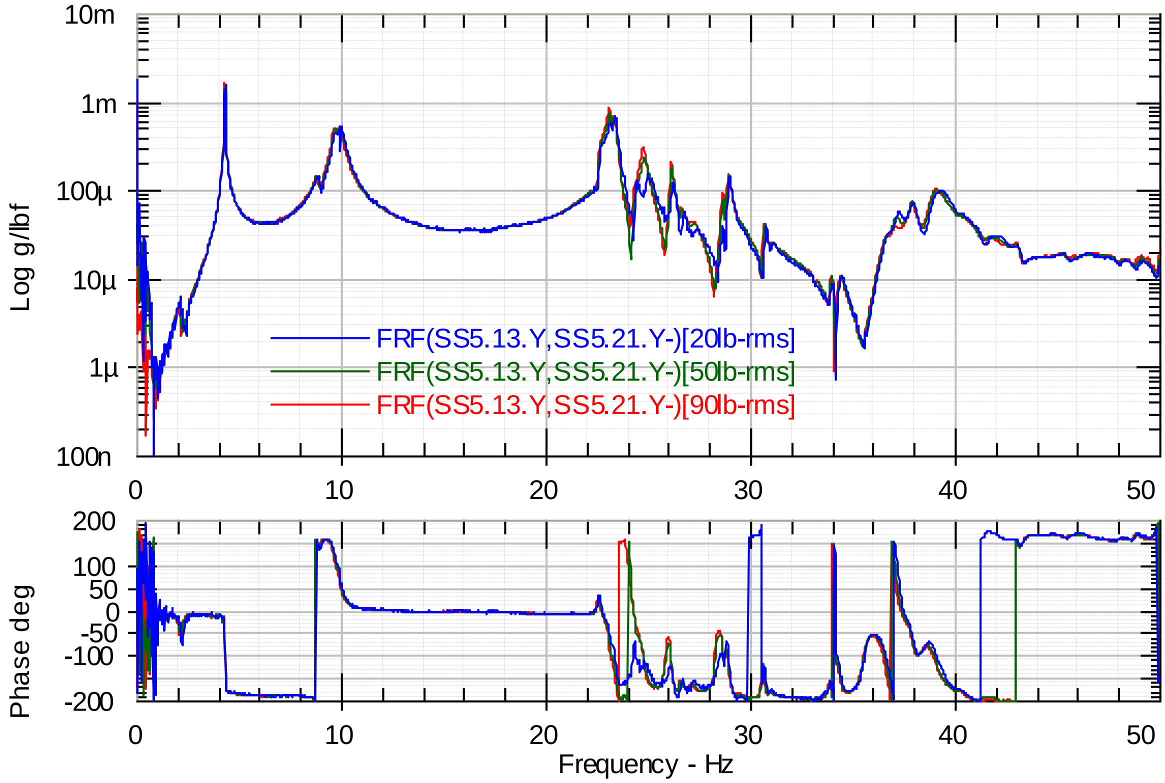

Figure 26 Y-direction FRFs from burst random tests SS5-6, SS5-8, and SS5-9

Table 4 Peak Frequency Variation for Random Excitation

Mode	Random 20 lb-rms Peak Frequency (Hz)	Random 90 lb-rms Peak Frequency (Hz)	Percent Difference (%)
1	4.19	4.19	0.00
2	4.34	4.31	0.73
3	8.94	8.84	1.06
4	10.03	9.94	0.94

4.4 Sine Sweep Data Analysis

Sine sweep tests were performed to evaluate the linearity of the response with respect to excitation level. One important parameter for obtaining useful results from a sine sweep is the sweep rate. Time histories of LAS tip acceleration for various sweep rates are shown in figure 27. Only portions of the 0.25 Hz/min and 0.5 Hz/min sweeps are shown in figure 27 so that they are properly scaled with respect to the 0.1 Hz/min sweep. As the sweep rate decreases, the structure is given more time to respond to the inputs, so the peak frequency comes closer to the actual steady state peak frequency of the desired mode. For the sweep through the 2nd mode frequency, a sweep rate of 0.1 Hz/min was selected. However, Ewins [7] recommends a sweep rate less than $216(f_n)^2(\zeta_n)^2$, which is 0.036 Hz/min for this particular mode. Sweeping up and down over the range of ±5% of the natural frequency would have required 28 minutes to complete, and multiple levels were required to investigate nonlinearity. Because of the short test schedule, the sweep rate of 0.1 Hz/min was chosen for this mode, requiring only 10 minutes for a sweep up and down. The resulting error in the peak frequency for mode 2 is less than 1% [8] with this sweep rate. Sweep rates for modes 3 and 4 were 0.2 Hz/min, which was slower than the recommended maximum rates defined by Ewins ($\leq 216\ (f_n)^2(\zeta_n)^2$) [7]. A representative time history from the 20 lb sine sweep for mode 4 is shown in Figure 28.

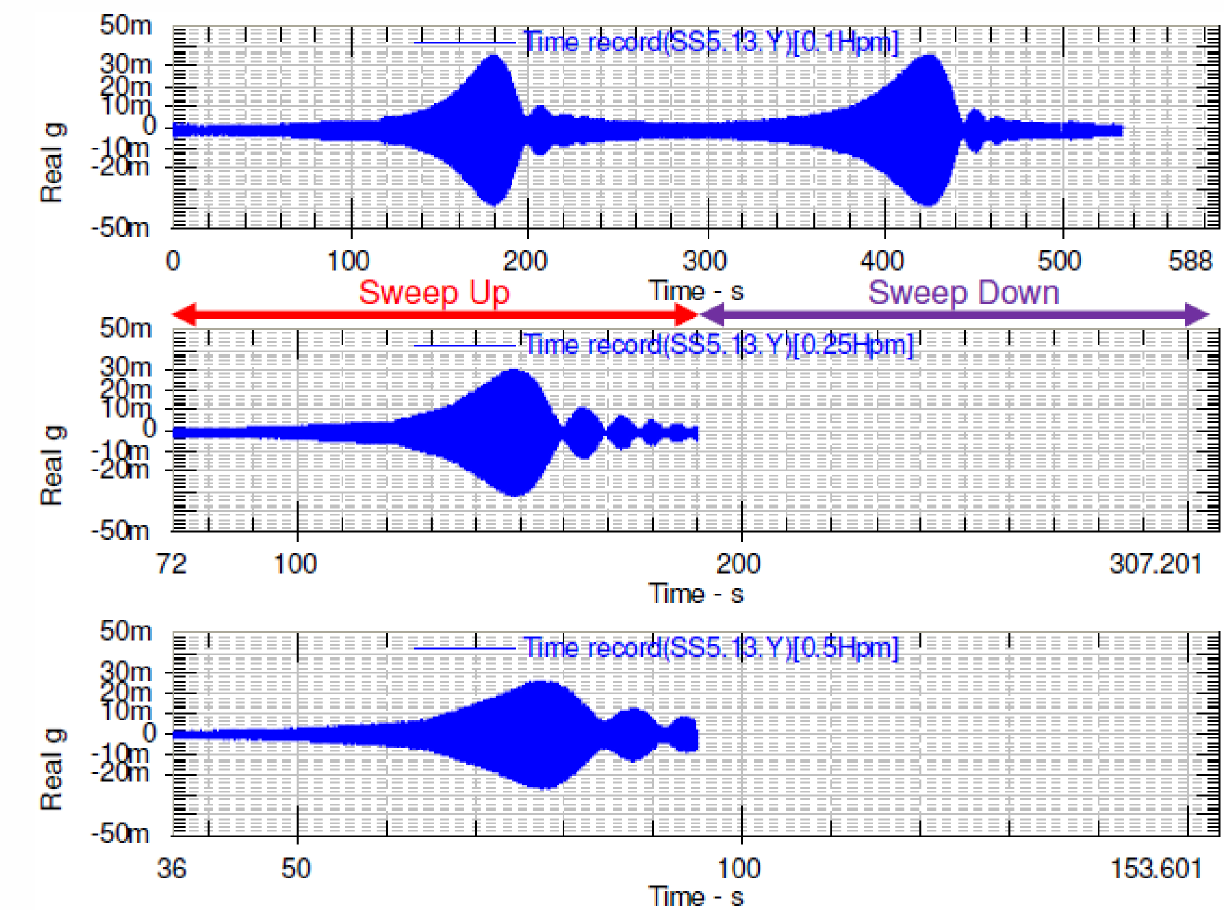

Figure 27 LAS tip acceleration for 20 lb-pk sine sweep on mode 2 at various sweep rates

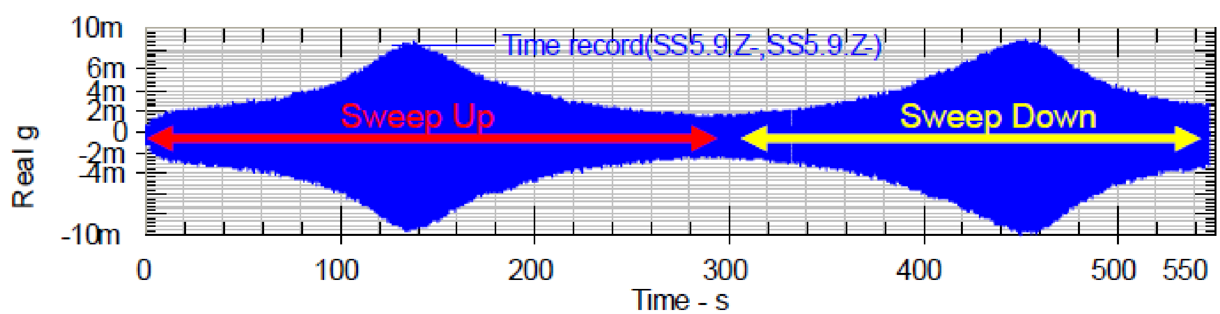

Figure 28 LAS tip acceleration for 20 lb-pk sine sweep on mode 4

To estimate FRFs from the sine sweeps, the time histories were split between sweeps up and down, and a single Discrete Fourier Transform (DFT) was taken of each. Because a single DFT block was used to process the data, the FRFs were estimated by a simple ratio of the acceleration spectra divided by the force spectrum. Figure 29 shows the FRF results from the 0.1 Hz/min upward sweeps for the 2nd mode at 20, 50, and 100 lb-pk, compared to the 90 lb-rms burst random FRF. As the force level increased, the frequency decreased, as indicated by the peaks moving to the left with increased force level. A comparison of the FRFs resulting from different sweep directions is shown in figure 30. It is interesting to note that although the FRF from the sweep down had a higher peak value, the peak frequency remained nearly identical.

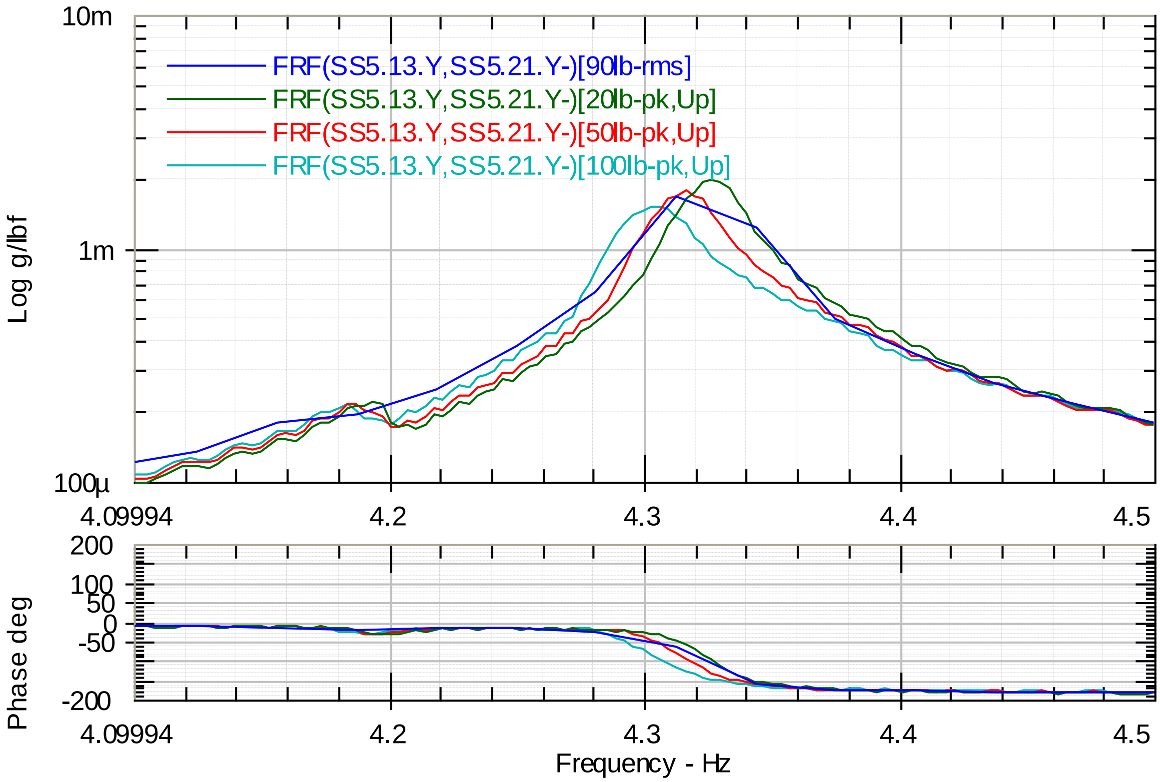

Figure 29 Variation in mode 2 response due to varying sine sweep levels

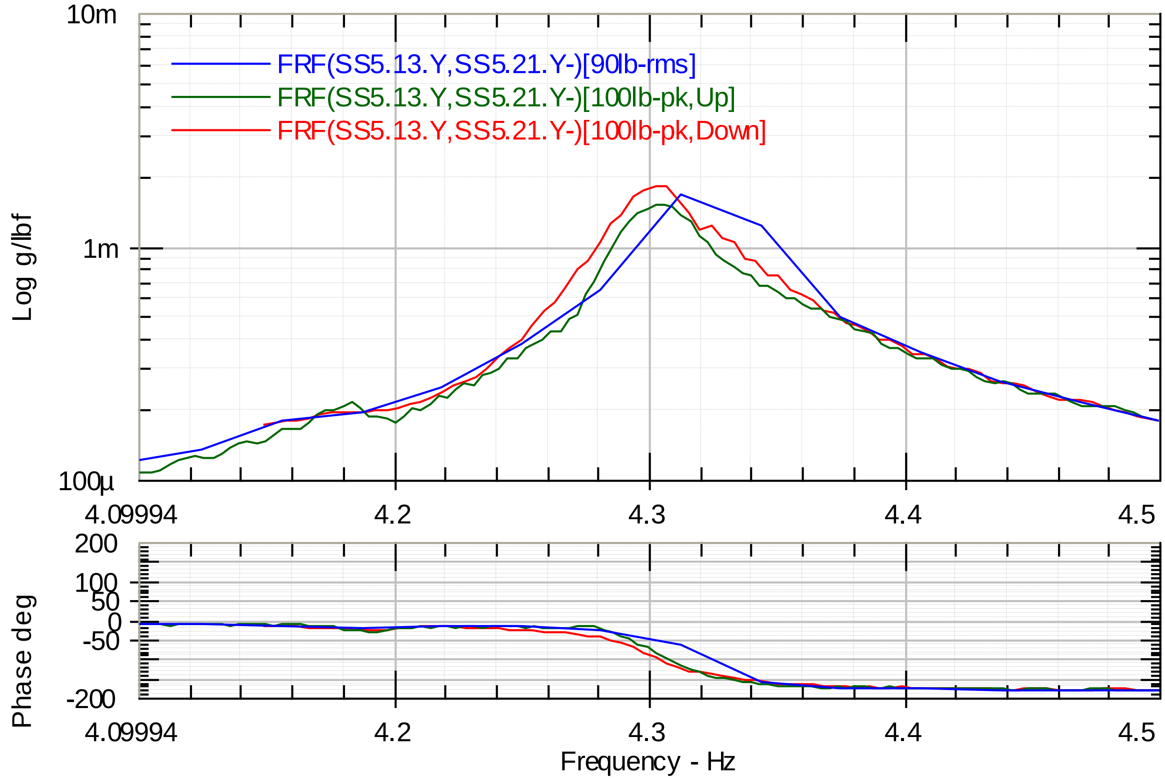

Figure 30 Variation in mode 2 response due to sweep direction

A similar approach was used to investigate modes 3 and 4. For these modes, the sweep rate was selected to be 0.2 Hz/min. Figures 31 and 32 show that these modes both decreased in frequency as the force level increased. For mode 4, all FRFs indicated two peaks of slightly different magnitude in the same frequency range. This was also seen in the burst random data and may be due to nonlinearities in the boundary associated with the gaps observed for some of the shims at the cart to floor interface.

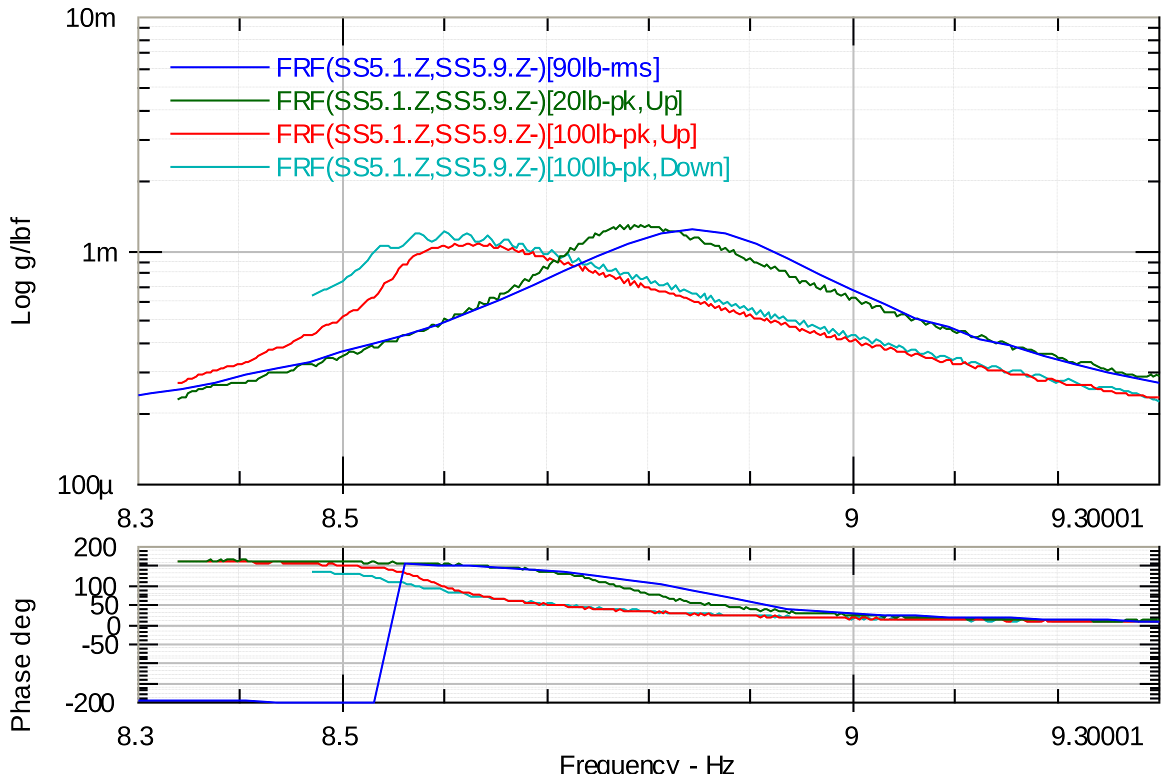

Figure 31 Variation in mode 3 response due to varying sine sweep levels

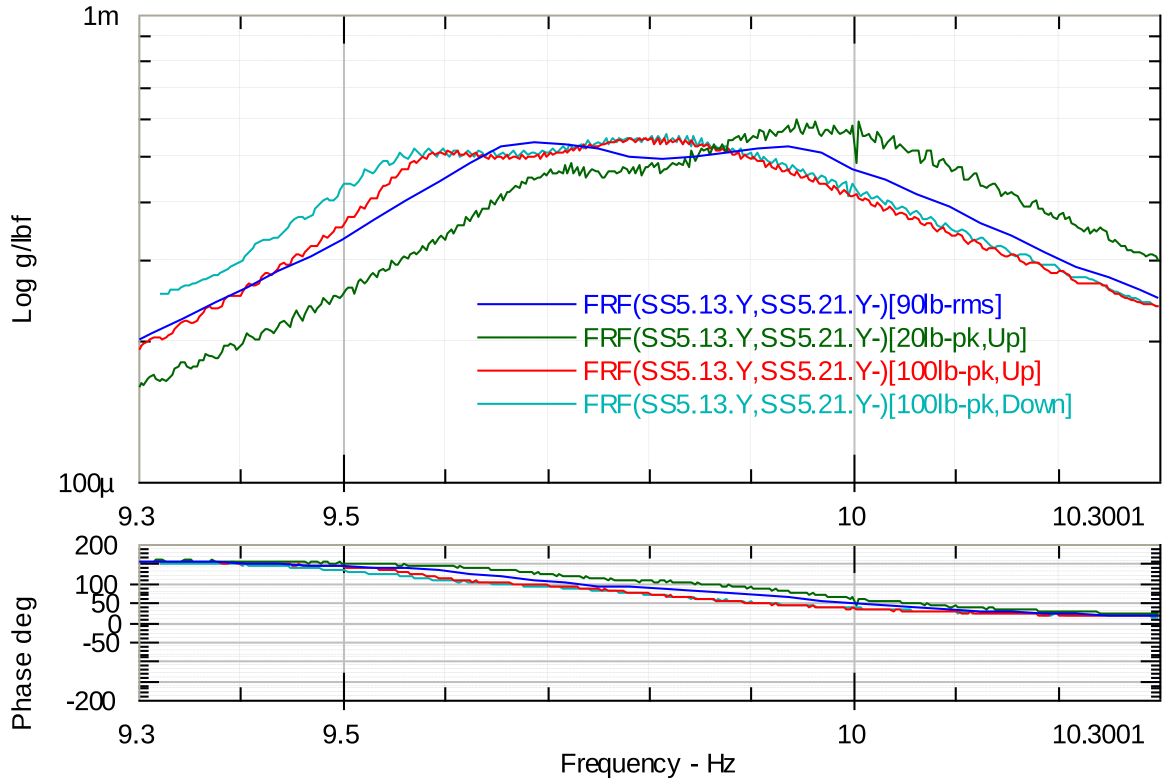

Figure 32 Variation in mode 4 response due to varying sine sweep levels

A summary of the sine sweep test results is given in table 5, which shows the peak frequencies at 20 lb-pk and 100 lb-pk force levels. The table shows that these modes did not vary more than 1.92% over the tested force range. Mode 1 is not included in the table because there was insufficient test time to complete another series of sine sweeps for that particular mode. The random tests indicated that mode 1 was the most linear of the modes, so further investigation was not necessary. As was described in the pre-test analysis, modes 3 and 4 (system bending) were most influenced by the boundary condition. These modes show more variation than the 2nd mode, which may be due to nonlinearities in the boundary interface. In any case, the variations observed are small and the system behaved fairly linearly over the tested force levels.

Table 5 Peak Frequency Variation Due to Sine Sweep Excitation Level

Mode	Sweep Up 20 lb-pk Peak Frequency (Hz)	Sweep Up 50 lb-pk Peak Frequency (Hz)	Sweep Up 100 lb-pk Peak Frequency (Hz)	20 vs. 100 lb-pk Percent Difference (%)
2	4.3265	4.3163	4.3027	-0.55
3	8.7799	n/a	8.6116	-1.92
4	9.9453	n/a	9.8150	-1.31

5.0 Experimental Modal Analysis Results

To verify that the telehandler did not affect the modal frequencies of the test article, the results of impact and burst random tests were compared. Figures 33 and 34 show sample FRFs from both test methods. The peak frequencies of the target modes are consistent for both tests methods, verifying that the shaker setup did not have a significant effect on the data. Differences in FRF characteristics near the peaks are attributed to the different excitation methods and data acquisition parameters. In comparison to the impact data, the burst random data provided higher averages, higher frequency resolution, higher signal to noise, and better control of the frequency range and level of excitation. Therefore, the burst random data is recommended for parameter estimation efforts.

Results of parameter estimation for the burst random data at 90 lb_{rms} (Test: SS5-9) are shown in Table 6. The corresponding mode shapes are shown in Appendix E. Each of the targeted mode pairs from the pre-test analysis (Table 1, Figure 4) is identified. However, the measured preferred directions of motion varied from those predicted. This is attributed to the symmetry of the structure. Although the measured bending modes are not on the Y- and Z-axis, as predicted, they still provide an orthogonal set that adequately describes the modal space. A test geometry file and final set of modes is included on the data archival DVD.

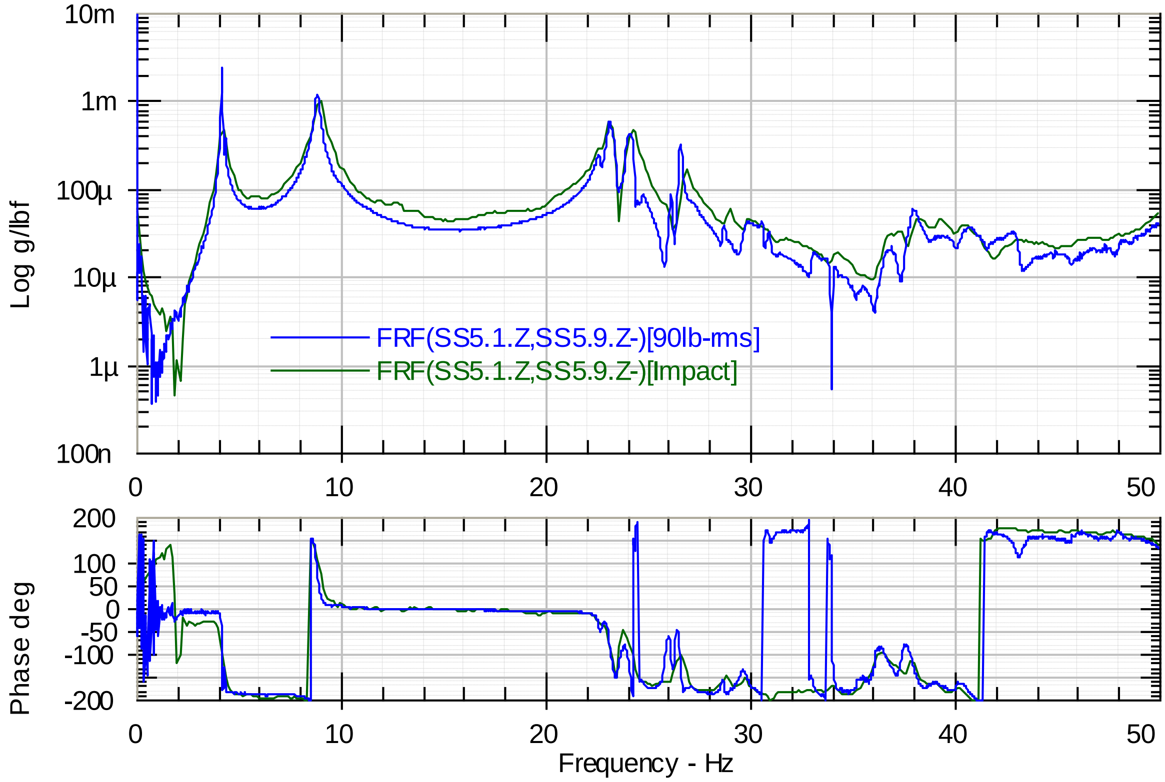

Figure 33 Z-direction FRFs from impact test and 90 lb-rms burst random test

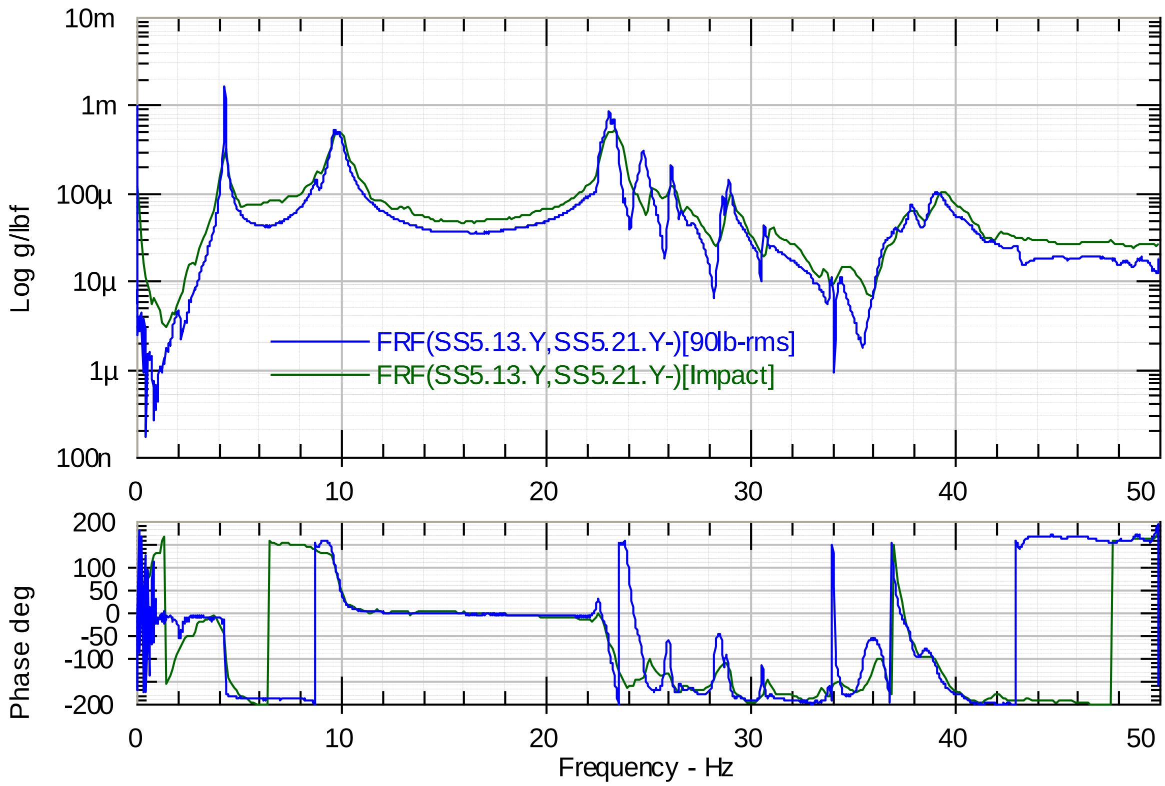

Figure 34 Y-direction FRFs from impact test and 90 lb-rms burst random test

Table 6 Experimental Modal Analysis Results; 90 lb_{rms} Burst Random Test

Mode	Frequency (Hz)	Damping (%)	Description
1	4.18	0.30	LAS 1st bending
2	4.32	0.33	LAS 1st bending
3	8.84	1.17	System bending
4	9.90	1.57	System bending
5	22.6	0.51	LAS 2nd bending
6	23.1	0.44	LAS 2nd bending

6.0 Comparison of Analysis and Test

A summary of the comparisons between the pre-test analysis and test data is provided. Details of the model calibration process can be found in Horta [9]. Initial pre-test analysis indicated significant discrepancies in the system bending mode frequencies as indicated in Table 7. After updating the boundary stiffness and correcting the LAS nozzle inertia properties based on measured mass properties, the first LAS bending mode pair that is critical for the flight test vehicle modes of interest was within 2.9%. Correlation of the 3rd through 6th mode frequencies was also greatly improved. As a means of comparing mode shapes, the cross-orthogonality with the test data is shown for the pre-test and updated model in Figures 35 and 36. When examining the orthogonality results recall that values range from 0 to 1 with 1 representing an exact match as indicated by the corresponding black square. It is clear that updates to the boundary stiffness not only reduced the frequency error but also helped correct for errors in the principal directions, as indicated by the reduced off-diagonal terms. After the sixth mode the orthogonality values quickly drop off, indicating an inability to capture the higher frequency modes with the test instrumentation set.

Table 7 Analysis/Test Frequency Comparison; 90 lb_{rms} Burst Random Test

Mode	Pre-Test FEM Frequency (Hz)	Updated FEM Frequency (Hz)	Test Frequency (Hz)	% Difference $(f_{\text{updated FEM}} - f_{\text{test}})/f_{\text{test}}*100$
1	4.60	4.30	4.18	2.9
2	4.68	4.38	4.32	1.4
3	12.19	8.73	8.84	-1.2
4	14.72	9.24	9.90	-6.7
5	26.06	25.04	23.1	8.4
6	26.25	25.12	22.6	11.2

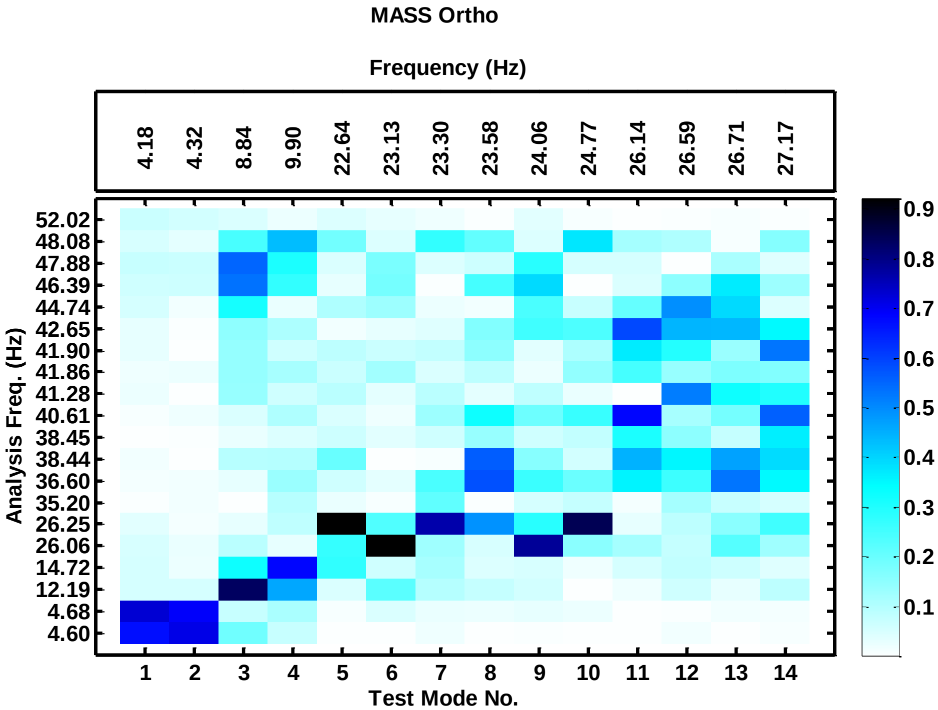

Figure 35 SS5 orthogonality results with pre-test model

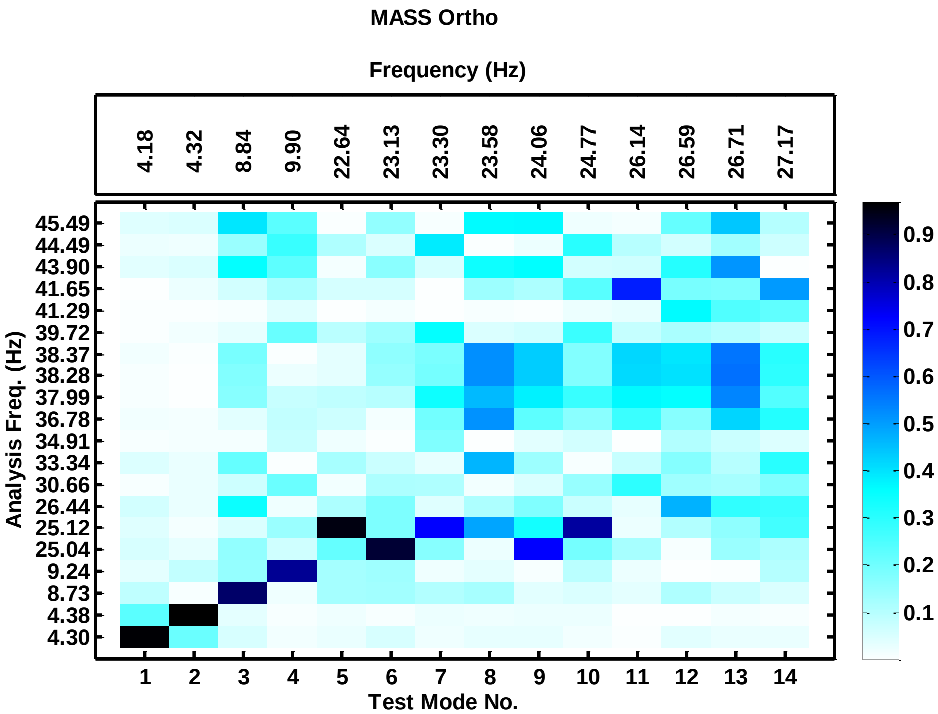

Figure 36 SS5 orthogonality results with optimized boundary parameters

7.0 Summary

The modal test successfully identified all of the targeted bending modes. Modal parameters were obtained using both multi-input burst random and impact excitations. Additionally, sine sweep tests were performed on the 2nd through 4th modes to investigate frequency nonlinearities. Results from multiple levels of random and sine sweep testing indicated a fairly linear response behavior, with maximum frequency shifts of 1.9% for over quadruple the force levels.

The FEM required updating of the boundary stiffness due to the unconventional test boundary with the systems resting on shims. An error in the inertias of the LAS nozzles was also identified and updated in the FEM. Further details on the model calibration can be found in Horta [9].

References:

[1] NASA Fact Sheet, Constellation Program: Ares I-X Flight Test Vehicle, FS-2009-03-007-JSC, 2009. http://www.nasa.gov/pdf/354470main_aresIX_fs_may09.pdf

[2] Buehrle, R. D., Templeton, J. D., Reaves, M. C., Horta, L. H., Bartolotta, P. A., Parks, R. A., Lazor, D. R., and Gaspar, J. L; Ares I-X Flight Test Vehicle Modal Test, NASA/TM-20xx-xxxxxx, Submitted December 2009

[3] Tuttle, R., and Lollock, J. A.; Modal Test Data Adjustment for Interface Compliance, Proceedings of IMAC XXVIII, Jacksonville, Florida, February 1-4, 2010.

[4] Tuttle, R., Lollock, J.A, and Hwung, J.S.: "Identifying Goals for Ares I-X Modal Testing," Proceedings of IMAC XXVIII, Jacksonville, FL., February 1-4, 2010.

[5] Kammer, D. C.; Sensor Placement for On-Orbit Modal Identification and Correlation of Large Space Structures, Journal of Guidance, Volume 14, No. 2, March-April 1991.

[6] Templeton, J. D., Buehrle, R. D., Parks, R. A., Lazor, D. R., and Gaspar, J. L.; Ares I-X Launch Vehicle Modal Test Measurements and Data Quality Assessments, Proceedings of IMAC XXVIII, Jacksonville, Florida, February 1-4, 2010.

[7] Ewins, D.J., Modal Testing: Theory, Practice and Application, 2nd Edition, Research Studies Press Ltd., pp. 231-234, 2000.

[8] Lollock, J. A., "The Effect of Swept Sinusoidal Excitation on the Response of a Single-Degree-of-Freedom Oscillator," 43rd AIAA/ASME/ASCE/AHS/ASC Structures, Structural Dynamics and Materials Conference, April 2002.

[9] Horta, L. H., Reaves, M. C., Buehrle, R. D., Templeton, J. D., Lazor, D. R., Gaspar, J. L., Parks, R. A., and Bartolotta, P. A..; Finite Element Model Calibration Approach for Ares I-X, Proceedings of IMAC XXVIII, Jacksonville, Florida, February 1-4, 2010.

Appendix A: Acronyms and Abbreviations

BNC	**(Bayonet Neill Concelman) coaxial cable connector**
CM	**Crew Module**
CS	**Coordinate System**
CDAS	**Critical Data Acquisition System**
DAS	**Data Acquisition System**
DFT	**Discrete Fourier Transform**
DOF	**Degree of Freedom**
FEM	**Finite Element Model**
FTINU	**Fault Tolerant Inertial Navigation Unit**
FRF	**Frequency Response Function**
FTV	**Flight Test Vehicle**
GRC	**Glenn Research Center**
GSE	**Ground Support Equipment**
HPS	**Hydraulic Power Supply**
Hz	**Hertz**
IEEE	**Institute of Electrical and Electronics Engineers**
IEPE	**Integrated Electronics Piezo Electric**
IPT's	**Integrated Product Teams**
IS	**Interstage**
IVM	**Integrated Vehicle Model**
HB	**High Bay**
KSC	**Kennedy Space Center**
LaRC	**Langley Research Center**
LAS	**Launch Abort System**
lb	**Pound**
LVDT	**Linear Variable Displacement Transducer**
MIMO	**Multi-Input Multi-Output**

MLP	**Mobile Launcher Platform**
MSFC	**Marshall Space Flight Center**
pk	**Peak**
psi	**Pounds per square inch**
PV	**Principal Value**
rms	**Root Mean Square**
RRGU	**Redundant Rate Gyro Unit**
SA	**Spacecraft Adapter**
SE&I	**Systems Engineering & Integration**
SM	**Service Module**
SSAS	**Super-Segment Assembly Stand**
STDev	**Standard Deviation**
STI	**Scientific and Technical Information**
TBD	**To Be Determined**
TBR	**To Be Resolved**
UPS	**U**ninterrupted **P**ower **S**upply
USS	**Upper Stage Simulator**
VAB	**Vehicle Assembly Building**
VXI	**VME eXtensions for Instrumentation**

Appendix B: Equipment List

Table B.1. Stack 5 Equipment List (1 of 3)

	DATA ACQUISITION SYSTEM (DAS) RACK							
NAME	**MANUFACTURER**	**MODEL**	**SERIAL**	**OWNER**	**QTY**	**CAL DATE**	**CAL DUE**	**MISC**
VXI MAINFRAME	AGILENT TECHNOLOGIES	E8403A	US38001676	LaRC	1	n/a	n/a	
SLOT-0 INTERFACE	AGILENT TECHNOLOGIES	E8491A	US39007039	LaRC	1	n/a	n/a	VXI 0
16 CHANNEL DIGITIZER	VXI TECHNOLOGY INC	VT1432B	US45004211	LaRC	1	8/17/2007	8/17/2009	VXI 1
16 CHANNEL DIGITIZER	VXI TECHNOLOGY INC	VT1432B	US45004212	LaRC	1	8/16/2007	8/16/2009	VXI 2
16 CHANNEL DIGITIZER	VXI TECHNOLOGY INC	VT1432B	US45004209	LaRC	1	8/16/2007	8/16/2009	VXI 3
16 CHANNEL DIGITIZER	VXI TECHNOLOGY INC	VT1432B	US45004210	LaRC	1	8/16/2007	8/16/2009	VXI 4
16 CHANNEL DIGITIZER	VXI TECHNOLOGY INC	VT1432B	US45004537	LaRC	1	1/22/2008	1/22/2010	VXI 5
16 CHANNEL DIGITIZER	VXI TECHNOLOGY INC	VT1432B	US45004538	LaRC	1	1/22/2008	1/22/2010	VXI 6
4 CHANNEL SOURCE MODULE	HEWLETT-PACKARD CO	E1434A	US37260104	LaRC	1	n/a	n/a	VXI 7
DIGITAL OSCILLOSCOPE	TEKTRONIX	TDS2014	C014678	LaRC	1	n/a	n/a	
ICP/VOLTAGE 8CH INPUT BOX	AGILENT TECHNOLOGIES	3241A	n/a	LaRC	4	n/a	n/a	
VOLTAGE 8CH INPUT BOX	HEWLETT-PACKARD CO	3240A	n/a	LaRC	4	n/a	n/a	
	SIGNAL CONDITIONER (S/C) RACK							
NAME	**MANUFACTURER**	**MODEL**	**SERIAL**	**OWNER**	**QTY**	**CAL DATE**	**CAL DUE**	**MISC**
ICP SIGNAL CONDITIONER	PCB PIEZOTRONICS	584A	1135	LaRC	1	2/9/2009	2/9/2010	S/C 1
CAPACITIVE SIGNAL CONDITIONER	PCB PIEZOTRONICS	478A16	151	LaRC	1	11/7/2008	11/7/2009	S/C 2
CAPACITIVE SIGNAL CONDITIONER	PCB PIEZOTRONICS	478A16	156	MSFC	1	3/10/2009	3/10/2010	S/C 3
CAPACITIVE SIGNAL CONDITIONER	PCB PIEZOTRONICS	478A16	154	MSFC	1	3/10/2009	3/10/2010	S/C 4
CAPACITIVE SIGNAL CONDITIONER	PCB PIEZOTRONICS	478A16	312	MSFC	1	1/12/2009	1/12/2010	S/C 5
CAPACITIVE SIGNAL CONDITIONER	PCB PIEZOTRONICS	478A16	157	MSFC	1	1/12/2009	1/12/2010	S/C 6
BANDPASS FILTER	KROHN-HITE	3343	2080	LaRC	1	4/20/2009	4/20/2011	
	ICP INSTRUMENTATION							
NAME	**MANUFACTURER**	**MODEL**	**SERIAL**	**OWNER**	**QTY**	**CAL DATE**	**CAL DUE**	**SENS**
IMPACT HAMMER	PCB PIEZOTRONICS	086B20	4095	LaRC	1	4/9/2009	4/9/2010	1.08 mV/lbf
TRIAXIAL ACCELEROMETER	PCB PIEZOTRONICS	356B21	89390x	MSFC	1	1/13/2009	1/13/2010	9.99 mV/g
|	|	|	89390y	MSFC	1	1/13/2009	1/13/2010	9.99 mV/g
V	V	V	89390z	MSFC	1	1/13/2009	1/13/2010	9.71 mV/g
TRIAXIAL ACCELEROMETER	PCB PIEZOTRONICS	356B21	89525x	MSFC	1	1/19/2009	1/19/2010	10 mV/g
|	|	|	89525y	MSFC	1	1/19/2009	1/19/2010	10.11 mV/g
V	V	V	89525z	MSFC	1	1/19/2009	1/19/2010	9.95 mV/g
IMPEDANCE HEAD	PCB PIEZOTRONICS	288M34	1785	MSFC	1	2/10/2009	2/10/2010	9.837 mV/lbf
V	V	V	1785	MSFC	1	2/10/2009	2/10/2010	99.0 mV/g
IMPEDANCE HEAD	PCB PIEZOTRONICS	288M34	1783	MSFC	1	2/10/2009	2/10/2010	9.915 mV/lbf
V	V	V	1783	MSFC	1	2/10/2009	2/10/2010	100.3 mV/g

Table B.1. Stack 5 Equipment List (2 of 3)

MSFC ACCELEROMETERS									
NAME	MANUFACTURER	MODEL	SERIAL	OWNER	QTY	CAL DATE	CAL DUE	159.2Hz SENS (mV/g)	DC SENS (mV/g)
CAPACITIVE ACCELEROMETER	PCB PIEZOTRONICS	3701M15	2562	MSFC	1	1/21/2009	1/21/2010	998	975
CAPACITIVE ACCELEROMETER	PCB PIEZOTRONICS	3701M15	2563	MSFC	1	1/21/2009	1/21/2010	1050	988
CAPACITIVE ACCELEROMETER	PCB PIEZOTRONICS	3701M15	2567	MSFC	1	1/22/2009	1/22/2010	1020	989
CAPACITIVE ACCELEROMETER	PCB PIEZOTRONICS	3701M15	2569	MSFC	1	1/21/2009	1/21/2010	1000	991
CAPACITIVE ACCELEROMETER	PCB PIEZOTRONICS	3701M15	2570	MSFC	1	1/21/2009	1/21/2010	964	980
CAPACITIVE ACCELEROMETER	PCB PIEZOTRONICS	3701M15	2571	MSFC	1	1/21/2009	1/21/2010	975	982
CAPACITIVE ACCELEROMETER	PCB PIEZOTRONICS	3701M15	2576	MSFC	1	1/21/2009	1/21/2010	991	975
CAPACITIVE ACCELEROMETER	PCB PIEZOTRONICS	3701M15	2577	MSFC	1	1/21/2009	1/21/2010	1050	989
CAPACITIVE ACCELEROMETER	PCB PIEZOTRONICS	3701M15	2578	MSFC	1	1/22/2009	1/22/2010	983	984
CAPACITIVE ACCELEROMETER	PCB PIEZOTRONICS	3701M15	2579	MSFC	1	1/21/2009	1/21/2010	1020	984
CAPACITIVE ACCELEROMETER	PCB PIEZOTRONICS	3701M15	2580	MSFC	1	1/21/2009	1/21/2010	1040	990
CAPACITIVE ACCELEROMETER	PCB PIEZOTRONICS	3701M15	2581	MSFC	1	1/21/2009	1/21/2010	1040	988
CAPACITIVE ACCELEROMETER	PCB PIEZOTRONICS	3701M15	2582	MSFC	1	1/21/2009	1/21/2010	1040	997
CAPACITIVE ACCELEROMETER	PCB PIEZOTRONICS	3701M15	2583	MSFC	1	1/21/2009	1/21/2010	1040	986
CAPACITIVE ACCELEROMETER	PCB PIEZOTRONICS	3701M15	2584	MSFC	1	1/22/2009	1/22/2010	1030	983
CAPACITIVE ACCELEROMETER	PCB PIEZOTRONICS	3701M15	2585	MSFC	1	1/22/2009	1/22/2010	996	992
CAPACITIVE ACCELEROMETER	PCB PIEZOTRONICS	3701M15	2586	MSFC	1	1/22/2009	1/22/2010	999	981
CAPACITIVE ACCELEROMETER	PCB PIEZOTRONICS	3701M15	2587	MSFC	1	1/21/2009	1/21/2010	1030	991
CAPACITIVE ACCELEROMETER	PCB PIEZOTRONICS	3701M15	2588	MSFC	1	1/22/2009	1/22/2010	1020	978
CAPACITIVE ACCELEROMETER	PCB PIEZOTRONICS	3701M15	2589	MSFC	1	1/21/2009	1/21/2010	979	983
CAPACITIVE ACCELEROMETER	PCB PIEZOTRONICS	3701M15	2591	MSFC	1	1/22/2009	1/22/2010	1040	990
CAPACITIVE ACCELEROMETER	PCB PIEZOTRONICS	3701M15	2592	MSFC	1	1/21/2009	1/21/2010	1040	986
CAPACITIVE ACCELEROMETER	PCB PIEZOTRONICS	3701M15	2595	MSFC	1	1/22/2009	1/22/2010	1010	995
CAPACITIVE ACCELEROMETER	PCB PIEZOTRONICS	3701M15	2596	MSFC	1	1/22/2009	1/22/2010	1040	988
CAPACITIVE ACCELEROMETER	PCB PIEZOTRONICS	3701M15	2597	MSFC	1	1/21/2009	1/21/2010	1040	997
CAPACITIVE ACCELEROMETER	PCB PIEZOTRONICS	3701M15	2598	MSFC	1	1/21/2009	1/21/2010	1020	1000
CAPACITIVE ACCELEROMETER	PCB PIEZOTRONICS	3701M15	2599	MSFC	1	1/21/2009	1/21/2010	974	991
CAPACITIVE ACCELEROMETER	PCB PIEZOTRONICS	3701M15	2601	MSFC	1	1/22/2009	1/22/2010	1000	988
CAPACITIVE ACCELEROMETER	PCB PIEZOTRONICS	3701M15	2603	MSFC	1	1/21/2009	1/21/2010	1030	984
CAPACITIVE ACCELEROMETER	PCB PIEZOTRONICS	3701M15	2605	MSFC	1	1/22/2009	1/22/2010	987	984
CAPACITIVE ACCELEROMETER	PCB PIEZOTRONICS	3701M15	2606	MSFC	1	1/22/2009	1/22/2010	1020	987
CAPACITIVE ACCELEROMETER	PCB PIEZOTRONICS	3701M15	2607	MSFC	1	1/22/2009	1/22/2010	1010	983
CAPACITIVE ACCELEROMETER	PCB PIEZOTRONICS	3701M15	2608	MSFC	1	1/22/2009	1/22/2010	1010	985
CAPACITIVE ACCELEROMETER	PCB PIEZOTRONICS	3701M15	2609	MSFC	1	1/21/2009	1/21/2010	1030	981
CAPACITIVE ACCELEROMETER	PCB PIEZOTRONICS	3701M15	2610	MSFC	1	1/22/2009	1/22/2010	1000	983
CAPACITIVE ACCELEROMETER	PCB PIEZOTRONICS	3701M15	2611	MSFC	1	1/21/2009	1/21/2010	1020	994
CAPACITIVE ACCELEROMETER	PCB PIEZOTRONICS	3701M15	2612	MSFC	1	1/21/2009	1/21/2010	1040	988
CAPACITIVE ACCELEROMETER	PCB PIEZOTRONICS	3701M15	2613	MSFC	1	1/21/2009	1/21/2010	1010	995
CAPACITIVE ACCELEROMETER	PCB PIEZOTRONICS	3701M15	2614	MSFC	1	1/22/2009	1/22/2010	1040	974
CAPACITIVE ACCELEROMETER	PCB PIEZOTRONICS	3701M15	2615	MSFC	1	1/22/2009	1/22/2010	1050	992
CAPACITIVE ACCELEROMETER	PCB PIEZOTRONICS	3701M15	2670	MSFC	1	1/22/2009	1/22/2010	1050	992
CAPACITIVE ACCELEROMETER	PCB PIEZOTRONICS	3701M15	2671	MSFC	1	1/22/2009	1/22/2010	1030	984
CAPACITIVE ACCELEROMETER	PCB PIEZOTRONICS	3701M15	2672	MSFC	1	1/21/2009	1/21/2010	991	986
CAPACITIVE ACCELEROMETER	PCB PIEZOTRONICS	3701M15	2673	MSFC	1	1/22/2009	1/22/2010	1030	985
CAPACITIVE ACCELEROMETER	PCB PIEZOTRONICS	3701M15	2675	MSFC	1	1/22/2009	1/22/2010	1030	988
CAPACITIVE ACCELEROMETER	PCB PIEZOTRONICS	3701M15	2676	MSFC	1	1/21/2009	1/21/2010	943	991
CAPACITIVE ACCELEROMETER	PCB PIEZOTRONICS	3701M15	2679	MSFC	1	1/22/2009	1/22/2010	1030	981
CAPACITIVE ACCELEROMETER	PCB PIEZOTRONICS	3701M15	8138	MSFC	1	1/21/2009	1/21/2010	1010	976
CAPACITIVE ACCELEROMETER	PCB PIEZOTRONICS	3701M15	8139	MSFC	1	1/21/2009	1/21/2010	985	977
CAPACITIVE ACCELEROMETER	PCB PIEZOTRONICS	3701M15	8140	MSFC	1	1/21/2009	1/21/2010	1060	1020
CAPACITIVE ACCELEROMETER	PCB PIEZOTRONICS	3701M15	8141	MSFC	1	1/21/2009	1/21/2010	1010	977
CAPACITIVE ACCELEROMETER	PCB PIEZOTRONICS	3701M15	8142	MSFC	1	1/21/2009	1/21/2010	1020	999
CAPACITIVE ACCELEROMETER	PCB PIEZOTRONICS	3701M15	8156	MSFC	1	1/21/2009	1/21/2010	941	990
CAPACITIVE ACCELEROMETER	PCB PIEZOTRONICS	3701M15	8157	MSFC	1	1/21/2009	1/21/2010	977	999

Table B.1. Stack 5 Equipment List (3 of 3)

CAPACITIVE ACCELEROMETER	PCB PIEZOTRONICS	3701M15	8158	MSFC	1	1/21/2009	1/21/2010	1010	987
CAPACITIVE ACCELEROMETER	PCB PIEZOTRONICS	3701M15	8159	MSFC	1	1/21/2009	1/21/2010	1010	997
CAPACITIVE ACCELEROMETER	PCB PIEZOTRONICS	3701M15	8160	MSFC	1	1/21/2009	1/21/2010	994	983
CAPACITIVE ACCELEROMETER	PCB PIEZOTRONICS	3701M15	8161	MSFC	1	1/21/2009	1/21/2010	932	980
CAPACITIVE ACCELEROMETER	PCB PIEZOTRONICS	3701M15	8162	MSFC	1	1/21/2009	1/21/2010	941	965
CAPACITIVE ACCELEROMETER	PCB PIEZOTRONICS	3701M15	8163	MSFC	1	1/21/2009	1/21/2010	1030	981
CAPACITIVE ACCELEROMETER	PCB PIEZOTRONICS	3701M15	8164	MSFC	1	1/21/2009	1/21/2010	972	1000
CAPACITIVE ACCELEROMETER	PCB PIEZOTRONICS	3701M15	8165	MSFC	1	1/21/2009	1/21/2010	986	980
CAPACITIVE ACCELEROMETER	PCB PIEZOTRONICS	3701M15	8166	MSFC	1	1/21/2009	1/21/2010	979	992
CAPACITIVE ACCELEROMETER	PCB PIEZOTRONICS	3701M15	8167	MSFC	1	1/21/2009	1/21/2010	1040	989
CAPACITIVE ACCELEROMETER	PCB PIEZOTRONICS	3701M15	8168	MSFC	1	1/21/2009	1/21/2010	998	984
CAPACITIVE ACCELEROMETER	PCB PIEZOTRONICS	3701M15	8169	MSFC	1	1/21/2009	1/21/2010	1040	990
CAPACITIVE ACCELEROMETER	PCB PIEZOTRONICS	3701M15	8170	MSFC	1	1/21/2009	1/21/2010	1010	981
CAPACITIVE ACCELEROMETER	PCB PIEZOTRONICS	3701M15	8171	MSFC	1	1/21/2009	1/21/2010	975	985
CAPACITIVE ACCELEROMETER	PCB PIEZOTRONICS	3701M15	8172	MSFC	1	1/22/2009	1/22/2010	981	984
CAPACITIVE ACCELEROMETER	PCB PIEZOTRONICS	3701M15	8173	MSFC	1	1/21/2009	1/21/2010	961	979
CAPACITIVE ACCELEROMETER	PCB PIEZOTRONICS	3701M15	8174	MSFC	1	1/21/2009	1/21/2010	951	972
CAPACITIVE ACCELEROMETER	PCB PIEZOTRONICS	3701M15	8175	MSFC	1	1/21/2009	1/21/2010	962	999
CAPACITIVE ACCELEROMETER	PCB PIEZOTRONICS	3701M15	8176	MSFC	1	1/21/2009	1/21/2010	929	984
CAPACITIVE ACCELEROMETER	PCB PIEZOTRONICS	3701M15	8177	MSFC	1	1/21/2009	1/21/2010	961	983
CAPACITIVE ACCELEROMETER	PCB PIEZOTRONICS	3701M15	8178	MSFC	1	1/21/2009	1/21/2010	1090	981
CAPACITIVE ACCELEROMETER	PCB PIEZOTRONICS	3701M15	8179	MSFC	1	1/21/2009	1/21/2010	978	980
CAPACITIVE ACCELEROMETER	PCB PIEZOTRONICS	3701M15	8180	MSFC	1	1/21/2009	1/21/2010	992	994
CAPACITIVE ACCELEROMETER	PCB PIEZOTRONICS	3701M15	8181	MSFC	1	1/21/2009	1/21/2010	1040	988
CAPACITIVE ACCELEROMETER	PCB PIEZOTRONICS	3701M15	8182	MSFC	1	1/21/2009	1/21/2010	1000	996
CAPACITIVE ACCELEROMETER	PCB PIEZOTRONICS	3711D1FA3G	517	MSFC	1	1/22/2009	1/22/2010	658	702
CAPACITIVE ACCELEROMETER	PCB PIEZOTRONICS	3711D1FA3G	518	MSFC	1	1/22/2009	1/22/2010	661	694
CAPACITIVE ACCELEROMETER	PCB PIEZOTRONICS	3711D1FA3G	519	MSFC	1	1/22/2009	1/22/2010	659	696
	LAS PRE-INSTALLED ACCELEROMETERS								
NAME	**MANUFACTURER**	**MODEL**	**SERIAL**	**OWNER**	**QTY**	**CAL DATE**	**CAL DUE**	**30Hz SENS (mV/g)**	**DC SENS (mV/g)**
CAPACITIVE ACCELEROMETER	PCB PIEZOTRONICS	3701G3FA3G	2020	LaRC	1	10/1/2008	10/1/2009	991.25	996.6
CAPACITIVE ACCELEROMETER	PCB PIEZOTRONICS	3701G3FA3G	2021	LaRC	1	9/29/2008	9/29/2009	998.74	1009.3
CAPACITIVE ACCELEROMETER	PCB PIEZOTRONICS	3701G3FA3G	2022	LaRC	1	10/1/2008	10/1/2009	998.93	995.9
CAPACITIVE ACCELEROMETER	PCB PIEZOTRONICS	3701G3FA3G	2023	LaRC	1	10/1/2008	10/1/2009	996.69	991.0
CAPACITIVE ACCELEROMETER	PCB PIEZOTRONICS	3701G3FA3G	2026	LaRC	1	9/29/2008	9/29/2009	993.12	991.0
CAPACITIVE ACCELEROMETER	PCB PIEZOTRONICS	3701G3FA3G	2027	LaRC	1	9/29/2008	9/29/2009	997.99	1003.9

Appendix C: Instrumentation Setup and Channel Mapping

Table C.1. Instrumentation Locations and Notes

	Installed Location		
Location	**X Station**	**Angle**	**Notes**
1	199	180	Pre-Installed in LAS
2	313.9	0	
3	382.6	0	
4	480.5	0	
5	565.2	180	Pre-Installed in LAS
6	631.6	0	
7	708.7	0	
8	816	0	
9	880.5	0	Shaker 1 location
10	943	0	
11	1041	0	
12	1068.3	0	
13	199.8	270	
14	313.9	270	
15	382.6	270	Y accelerometer was switched from 8172 to 2563 before SS5-7 test
16	480.5	270	
17	602	270	
18	631.6	270	
19	708.7	270	
20	816.1	270	
21	880	270	Shaker 2 location
22	995	270	
23	995	90	
24	995	180	
25	1069.5	0	
26	1069.5	267	
27	1069.5	85	
28	1069.5	180	
29	400.2	180	Pre-Installed in LAS
30	995	0	
31	874	5	Impedance head accelerometer at location 9
32	874	275	Impedance head accelerometer at location 21
33	-	-	Triaxial accelerometer mounted to shaker at location 9
34	-	-	Triaxial accelerometer mounted to shaker at location 21

Table C.2. Instrumentation Orientations

	X-Axis Accel		Y-Axis Accel		Z-Axis Accel		Load Cell	
Location	Orientation	S/N	Orientation	S/N	Orientation	S/N	Orientation	S/N
1			-Y	2020	-Z	2021		
2			Y	2608	Z	2610		
3			Y	2595	Z	2588		
4			Y	2585	Z	2607		
5			-Y	2026	-Z	2027		
6			Y	2606	Z	2605		
7			Y	2584	Z	2601		
8			Y	8171	-Z	8156		
9			Y	8164	-Z	8140	-Z	1783
10			Y	8168	-Z	8159		
11	-X	2603	Y	8177	Z	2577		
12	-X	2599	Y	2582	Z	8157		
13			Y	2586	Z	2578		
14			Y	2675	Z	2596		
15			Y	2563	Z	2615		
16			Y	2614	Z	2673		
17			Y	2679	Z	2591		
18			Y	2671	Z	2676		
19			Y	2751	Z	2567		
20			-Y	8169	Z	8179		
21			-Y	8161	Z	8176	-Y	1785
22	-X	8139	-Y	8181	Z	2569		
23	-X	2579	Y	8138	Z	8167		
24	-X	8160	Y	2562	Z	8142		
25	-X	8163	Y	2570	Z	2576		
26	-X	8166	Y	2597	Z	8180		
27	-X	2609	Y	2598	Z	2583		
28	-X	8178	Y	2587	Z	8165		
29			-Y	2022	-Z	2023		
30	-X	8162	Y	8141	-Z	8158		
31					Z	1783		
32			Y	1785				
33	X	89390	Y	89390	Z	89390		
34	X	89525	Y	89525	Z	89525		

Table C.4. Transducer Channel Setup (1 of 2)

TRANSDUCER CHANNELS								
Channel	**Usage**	**Name**	**EU**	**Sensitivity**	**Cal Type**	**Input Mode**	**Model**	**Serial**
1	Excitation	SS5.9.Z-	lbf	9.915	mV/EU	Voltage	288M34	1783
2	Excitation	SS5.21.Y-	lbf	9.837	mV/EU	Voltage	288M34	1785
3	Response	SS5.9.Z-	g	1020.0	mV/EU	Voltage	3701M15	8140
4	Response	SS5.21.Y-	g	980.0	mV/EU	Voltage	3701M15	8161
5	Response	SS5.2.Y	g	985.0	mV/EU	Voltage	3701M15	2608
6	Response	SS5.2.Z	g	983.0	mV/EU	Voltage	3701M15	2610
7	Response	SS5.3.Y	g	995.0	mV/EU	Voltage	3701M15	2595
8	Response	SS5.3.Z	g	978.0	mV/EU	Voltage	3701M15	2588
9	Response	SS5.4.Y	g	992.0	mV/EU	Voltage	3701M15	2585
10	Response	SS5.4.Z	g	983.0	mV/EU	Voltage	3701M15	2607
11	Response	SS5.6.Y	g	987.0	mV/EU	Voltage	3701M15	2606
12	Response	SS5.6.Z	g	984.0	mV/EU	Voltage	3701M15	2605
13	Response	SS5.7.Y	g	983.0	mV/EU	Voltage	3701M15	2584
14	Response	SS5.7.Z	g	988.0	mV/EU	Voltage	3701M15	2601
15	Response	SS5.8.Y	g	985.0	mV/EU	Voltage	3701M15	8171
16	Response	SS5.8.Z-	g	990.0	mV/EU	Voltage	3701M15	8156
17	Response	SS5.9.Y	g	1000.0	mV/EU	Voltage	3701M15	8164
18	Response	SS5.10.Y	g	984.0	mV/EU	Voltage	3701M15	8168
19	Response	SS5.10.Z-	g	997.0	mV/EU	Voltage	3701M15	8159
20	Response	SS5.11.Y	g	983.0	mV/EU	Voltage	3701M15	8177
21	Response	SS5.11.Z	g	989.0	mV/EU	Voltage	3701M15	2577
22	Response	SS5.12.X-	g	991.0	mV/EU	Voltage	3701M15	2599
23	Response	SS5.12.Y	g	997.0	mV/EU	Voltage	3701M15	2582
24	Response	SS5.12.Z	g	999.0	mV/EU	Voltage	3701M15	8157
25	Response	SS5.13.Y	g	981.0	mV/EU	Voltage	3701M15	2586
26	Response	SS5.13.Z	g	984.0	mV/EU	Voltage	3701M15	2578
27	Response	SS5.14.Y	g	988.0	mV/EU	Voltage	3701M15	2675
28	Response	SS5.14.Z	g	988.0	mV/EU	Voltage	3701M15	2596
29	Inactive		g	988.0	mV/EU	Voltage		
30	Response	SS5.15.Z	g	992.0	mV/EU	Voltage	3701M15	2615
31	Response	SS5.16.Y	g	974.0	mV/EU	Voltage	3701M15	2614
32	Response	SS5.16.Z	g	985.0	mV/EU	Voltage	3701M15	2673
33	Response	SS5.17.Y	g	981.0	mV/EU	Voltage	3701M15	2679
34	Response	SS5.17.Z	g	990.0	mV/EU	Voltage	3701M15	2591
35	Response	SS5.18.Y	g	984.0	mV/EU	Voltage	3701M15	2671
36	Response	SS5.18.Z	g	991.0	mV/EU	Voltage	3701M15	2676
37	Response	SS5.19.Y	g	982.0	mV/EU	Voltage	3701M15	2571
38	Response	SS5.19.Z	g	989.0	mV/EU	Voltage	3701M15	2567
39	Response	SS5.20.Y-	g	990.0	mV/EU	Voltage	3701M15	8169
40	Response	SS5.20.Z	g	980.0	mV/EU	Voltage	3701M15	8179

Table C.4. Transducer Channel Setup (2 of 2)

TRANSDUCER CHANNELS								
Channel	Usage	Name	EU	Sensitivity	Cal Type	Input Mode	Model	Serial
41	Response	SS5.21.Z	g	984.0	mV/EU	Voltage	3701M15	8176
42	Response	SS5.22.X-	g	977.0	mV/EU	Voltage	3701M15	8139
43	Response	SS5.22.Y-	g	988.0	mV/EU	Voltage	3701M15	8181
44	Response	SS5.22.Z	g	991.0	mV/EU	Voltage	3701M15	2569
45	Response	SS5.23.X-	g	984.0	mV/EU	Voltage	3701M15	2579
46	Response	SS5.23.Y	g	976.0	mV/EU	Voltage	3701M15	8138
47	Response	SS5.23.Z	g	989.0	mV/EU	Voltage	3701M15	8167
48	Response	SS5.24.X-	g	983.0	mV/EU	Voltage	3701M15	8160
49	Response	SS5.24.Y	g	975.0	mV/EU	Voltage	3701M15	2562
50	Response	SS5.24.Z	g	999.0	mV/EU	Voltage	3701M15	8142
51	Response	SS5.25.X-	g	981.0	mV/EU	Voltage	3701M15	8163
52	Response	SS5.25.Y	g	980.0	mV/EU	Voltage	3701M15	2570
53	Response	SS5.25.Z	g	975.0	mV/EU	Voltage	3701M15	2576
54	Response	SS5.26.X-	g	992.0	mV/EU	Voltage	3701M15	8166
55	Response	SS5.26.Y	g	997.0	mV/EU	Voltage	3701M15	2597
56	Response	SS5.26.Z	g	994.0	mV/EU	Voltage	3701M15	8180
57	Response	SS5.27.X-	g	981.0	mV/EU	Voltage	3701M15	2609
58	Response	SS5.27.Y	g	1000.0	mV/EU	Voltage	3701M15	2598
59	Response	SS5.27.Z	g	986.0	mV/EU	Voltage	3701M15	2583
60	Response	SS5.28.X-	g	981.0	mV/EU	Voltage	3701M15	8178
61	Response	SS5.28.Y	g	991.0	mV/EU	Voltage	3701M15	2587
62	Response	SS5.28.Z	g	980.0	mV/EU	Voltage	3701M15	8165
63	Response	SS5.1.Y-	g	996.6	mV/EU	Voltage	3701G3FA3G	2020
64	Response	SS5.1.Z	g	1009.3	mV/EU	Voltage	3701G3FA3G	2021
65	Response	SS5.5.Y-	g	991.0	mV/EU	Voltage	3701G3FA3G	2026
66	Response	SS5.5.Z	g	1003.9	mV/EU	Voltage	3701G3FA3G	2027
67	Response	SS5.29.Y-	g	995.9	mV/EU	Voltage	3701G3FA3G	2022
68	Response	SS5.29.Z	g	991.0	mV/EU	Voltage	3701G3FA3G	2023
69	Response	SS5.31.Z	g	100.3	mV/EU	Voltage	288M34	1783
70	Response	SS5.32.Y	g	99.0	mV/EU	Voltage	288M34	1785
71	Response	SS5.33.X	g	9.99	mV/EU	Voltage	356B21	89390
72	Response	SS5.33.Y	g	9.99	mV/EU	Voltage	356B21	89390
73	Response	SS5.33.Z	g	9.71	mV/EU	Voltage	356B21	89390
74	Response	SS5.34.X	g	10.00	mV/EU	Voltage	356B21	89525
75	Response	SS5.34.Y	g	10.11	mV/EU	Voltage	356B21	89525
76	Response	SS5.34.Z	g	9.95	mV/EU	Voltage	356B21	89525
77	Response	SS5.11.X-	g	984.0	mV/EU	Voltage	3701M15	2603
78	Response	SS5.30.X-	g	965.0	mV/EU	Voltage	3701M15	8162
79	Response	SS5.30.Y	g	977.0	mV/EU	Voltage	3701M15	8141
80	Response	SS5.30.Z-	g	987.0	mV/EU	Voltage	3701M15	8158
81	Response	SS5.15.Y	g	988.0	mV/EU	Voltage	3701M15	2563

Table C.5. Acquisition Channel Setup (1 of 2)

	INPUT CHANNELS				
Channel	Coupling	Range	Offset	Pre-gain	Weighting
1	DC Gnd	10 V	0	1	Off
2	DC Gnd	10 V	0	1	Off
3	DC Gnd	10 V	0	1	Off
4	DC Gnd	10 V	0	1	Off
5	DC Gnd	10 V	0	1	Off
6	DC Gnd	10 V	0	1	Off
7	DC Gnd	10 V	0	1	Off
8	DC Gnd	10 V	0	1	Off
9	DC Gnd	10 V	0	1	Off
10	DC Gnd	10 V	0	1	Off
11	DC Gnd	10 V	0	1	Off
12	DC Gnd	10 V	0	1	Off
13	DC Gnd	10 V	0	1	Off
14	DC Gnd	10 V	0	1	Off
15	DC Gnd	10 V	0	1	Off
16	DC Gnd	10 V	0	1	Off
17	DC Gnd	10 V	0	1	Off
18	DC Gnd	10 V	0	1	Off
19	DC Gnd	10 V	0	1	Off
20	DC Gnd	10 V	0	1	Off
21	DC Gnd	10 V	0	1	Off
22	DC Gnd	10 V	0	1	Off
23	DC Gnd	10 V	0	1	Off
24	DC Gnd	10 V	0	1	Off
25	DC Gnd	10 V	0	1	Off
26	DC Gnd	10 V	0	1	Off
27	DC Gnd	10 V	0	1	Off
28	DC Gnd	10 V	0	1	Off
29	DC Gnd	10 V	0	1	Off
30	DC Gnd	10 V	0	1	Off
31	DC Gnd	10 V	0	1	Off
32	DC Gnd	10 V	0	1	Off
33	DC Gnd	10 V	0	1	Off
34	DC Gnd	10 V	0	1	Off
35	DC Gnd	10 V	0	1	Off
36	DC Gnd	10 V	0	1	Off
37	DC Gnd	10 V	0	1	Off
38	DC Gnd	10 V	0	1	Off
39	DC Gnd	10 V	0	1	Off
40	DC Gnd	10 V	0	1	Off

Table C.5. Acquisition Channel Setup (2 of 2)

	INPUT CHANNELS				
Channel	Coupling	Range	Offset	Pre-gain	Weighting
41	DC Gnd	10 V	0	1	Off
42	DC Gnd	10 V	0	1	Off
43	DC Gnd	10 V	0	1	Off
44	DC Gnd	10 V	0	1	Off
45	DC Gnd	10 V	0	1	Off
46	DC Gnd	10 V	0	1	Off
47	DC Gnd	10 V	0	1	Off
48	DC Gnd	10 V	0	1	Off
49	DC Gnd	10 V	0	1	Off
50	DC Gnd	10 V	0	1	Off
51	DC Gnd	10 V	0	1	Off
52	DC Gnd	10 V	0	1	Off
53	DC Gnd	10 V	0	1	Off
54	DC Gnd	10 V	0	1	Off
55	DC Gnd	10 V	0	1	Off
56	DC Gnd	10 V	0	1	Off
57	DC Gnd	10 V	0	1	Off
58	DC Gnd	10 V	0	1	Off
59	DC Gnd	10 V	0	1	Off
60	DC Gnd	10 V	0	1	Off
61	DC Gnd	10 V	0	1	Off
62	DC Gnd	10 V	0	1	Off
63	DC Gnd	10 V	0	1	Off
64	DC Gnd	10 V	0	1	Off
65	DC Gnd	10 V	0	1	Off
66	DC Gnd	10 V	0	1	Off
67	DC Gnd	10 V	0	1	Off
68	DC Gnd	10 V	0	1	Off
69	DC Gnd	10 V	0	1	Off
70	DC Gnd	10 V	0	1	Off
71	DC Gnd	10 V	0	1	Off
72	DC Gnd	10 V	0	1	Off
73	DC Gnd	10 V	0	1	Off
74	DC Gnd	10 V	0	1	Off
75	DC Gnd	10 V	0	1	Off
76	DC Gnd	10 V	0	1	Off
77	DC Gnd	10 V	0	1	Off
78	DC Gnd	10 V	0	1	Off
79	DC Gnd	10 V	0	1	Off
80	DC Gnd	10 V	0	1	Off
81	DC Gnd	10 V	0	1	Off

Table C.6. Channel Connectivity (1 of 2)

	SIGNAL CONDITIONER CHANNELS					PATCH PANEL			VXI CHANNELS	
Channel	**Box**	**Channel**	**Type**	**Cable**	**Connector**	**Box**	**Channel**		**Card**	**Group**
1	1	1	ICP	BNC		1	1		1	1
2	1	2	ICP	BNC		1	2		1	1
3	2	3	Capacitive	BNC		1	3		1	1
4	2	4	Capacitive	BNC		1	4		1	1
5	2	5	Capacitive	Agilent	2				1	2
6	2	6	Capacitive	Agilent	2				1	2
7	2	7	Capacitive	Agilent	2				1	2
8	2	8	Capacitive	Agilent	2				1	2
9	2	9	Capacitive	Agilent	3				1	3
10	2	10	Capacitive	Agilent	3				1	3
11	2	11	Capacitive	Agilent	3				1	3
12	2	12	Capacitive	Agilent	3				1	3
13	2	13	Capacitive	Agilent	4				1	4
14	2	14	Capacitive	Agilent	4				1	4
15	2	15	Capacitive	Agilent	4				1	4
16	2	16	Capacitive	Agilent	4				1	4
17	3	1	Capacitive	Agilent	1				2	1
18	3	2	Capacitive	Agilent	1				2	1
19	3	3	Capacitive	Agilent	1				2	1
20	3	4	Capacitive	Agilent	1				2	1
21	3	5	Capacitive	Agilent	2				2	2
22	3	6	Capacitive	Agilent	2				2	2
23	3	7	Capacitive	Agilent	2				2	2
24	3	8	Capacitive	Agilent	2				2	2
25	3	9	Capacitive	Agilent	3				2	3
26	3	10	Capacitive	Agilent	3				2	3
27	3	11	Capacitive	Agilent	3				2	3
28	3	12	Capacitive	Agilent	3				2	3
29	3	13	Capacitive	Agilent	4				2	4
30	3	14	Capacitive	Agilent	4				2	4
31	3	15	Capacitive	Agilent	4				2	4
32	3	16	Capacitive	Agilent	4				2	4
33	4	1	Capacitive	Agilent	1				3	1
34	4	2	Capacitive	Agilent	1				3	1
35	4	3	Capacitive	Agilent	1				3	1
36	4	4	Capacitive	Agilent	1				3	1
37	4	5	Capacitive	Agilent	2				3	2
38	4	6	Capacitive	Agilent	2				3	2
39	4	7	Capacitive	Agilent	2				3	2
40	4	8	Capacitive	Agilent	2				3	2

Table C.6. Channel Connectivity (2 of 2)

TRANSDU	SIGNAL CONDITIONER CHANNELS					PATCH PANEL			VXI CHANNELS	
Channel	Box	Channel	Type	Cable	Connector	Box	Channel		Card	Group
41	4	9	Capacitive	Agilent	3				3	3
42	4	10	Capacitive	Agilent	3				3	3
43	4	11	Capacitive	Agilent	3				3	3
44	4	12	Capacitive	Agilent	3				3	3
45	4	13	Capacitive	Agilent	4				3	4
46	4	14	Capacitive	Agilent	4				3	4
47	4	15	Capacitive	Agilent	4				3	4
48	4	16	Capacitive	Agilent	4				3	4
49	5	1	Capacitive	Agilent	1				4	1
50	5	2	Capacitive	Agilent	1				4	1
51	5	3	Capacitive	Agilent	1				4	1
52	5	4	Capacitive	Agilent	1				4	1
53	5	5	Capacitive	Agilent	2				4	2
54	5	6	Capacitive	Agilent	2				4	2
55	5	7	Capacitive	Agilent	2				4	2
56	5	8	Capacitive	Agilent	2				4	2
57	5	9	Capacitive	Agilent	3				4	3
58	5	10	Capacitive	Agilent	3				4	3
59	5	11	Capacitive	Agilent	3				4	3
60	5	12	Capacitive	Agilent	3				4	3
61	5	13	Capacitive	BNC		2	1		4	4
62	5	14	Capacitive	BNC		2	2		4	4
63	6	1	Capacitive	BNC		2	3		4	4
64	6	2	Capacitive	BNC		2	4		4	4
65	6	3	Capacitive	BNC		2	5		5	1
66	6	4	Capacitive	BNC		2	6		5	1
67	6	5	Capacitive	BNC		2	7		5	1
68	6	6	Capacitive	BNC		2	8		5	1
69	1	3	ICP	BNC		1	5		5	2
70	1	4	ICP	BNC		1	6		5	2
71	1	5	ICP	BNC		1	7		5	2
72	1	6	ICP	BNC		1	8		5	2
73	1	7	ICP	BNC		3	1		5	3
74	1	8	ICP	BNC		3	2		5	3
75	1	9	ICP	BNC		3	3		5	3
76	1	10	ICP	BNC		3	4		5	3
77	2	1	Capacitive	BNC		3	5		5	4
78	2	2	Capacitive	BNC		3	6		5	4
79	5	15	Capacitive	BNC		3	7		5	4
80	5	16	Capacitive	BNC		3	8		5	4
81	6	1	Capacitive	BNC		4	1		6	1

Appendix D: Data Acquisition Log

Pre-Test Setup and Checkout

SS5-1: May 26, 2009; Ambient noise data, 128 Hz sample rate, 0.03125 Hz resolution, 20 blocks; Umbilical cover installed but not all bolts installed; impedance sensors and shaker accelerometers not installed

Note that SS5-2 was conducted out of chronological order

SS5-3: May 26, 2009; Impact data (16Y-, 4Z-, 9Z-), 128 Hz sample rate, 8 second block, 0. 125 Hz resolution, 5 averages, 10% force window, 100% (Uniform) response window; Umbilical cover installed but not all bolts installed; impedance sensors and shaker accelerometers not installed; need to check data for possible saturation of accelerometers near drive point; only frequency domain data stored

SS5-4: May 27, 2009; Impact data (21Y-), 128 Hz sample rate, 8 second block, 0. 125 Hz resolution, 5 averages, 10% force window, 100% (Uniform) response window; Umbilical cover installed but not all bolts installed; impedance sensors and shaker accelerometers not installed; only frequency domain data stored

SS5-2: May 27, 2009; Ambient noise data, 128 Hz sample rate, 0.03125 Hz resolution, 20 blocks; fans shutdown, no work in bay; impedance sensors and shaker accelerometers not installed

Test Day

Shaker setup and installation; May 29, 2009 (7:30 AM- Noon); shakers centered 12 inches above SA/SM interface; Shaker 1 (9Z-) 5 degree angle; Shaker 2 (21Y-) 275 degree angle

SS5-5: May 29, 2009 (~1:30 pm start); Burst random (9Z-, 21Y-), 75% burst, ~8 lb-rms; 128 Hz sample rate, 0.03 125 Hz resolution, 20 averages, uniform window; response of LAS accelerometers does not decay fully in sample period—need to reduce burst percentage

SS5-6: May 29, 2009 (~2:34 pm start); Burst random (9Z-, 21Y-), 50% burst, ~20 lb-rms; 128 Hz sample rate, 0.03 125 Hz resolution, 20 averages, uniform window; 15Y identified as bad channel –cable and transducer replaced (newe transducer S/N 2563, 988 mv/g)

SS5-7: May 29, 2009 (~3:15 pm start); Burst random (9Z-, 21Y-), 50% burst, ~20 lb-rms; 128 Hz sample rate, 0.03 125 Hz resolution, 40 averages, uniform window; 15Y out again—Amplifier #3 channel 13 bad (VXI channel 29)—rerouted to VXI channel 81

SS5-8: May 29, 2009 (~4:24 pm start); Burst random (9Z-, 21Y-), 50% burst, ~50 lb-rms; 128 Hz sample rate, 0.03 125 Hz resolution, 40 averages, uniform window; Noticeable audible rattle internal—“thunder” sound

SS5-9: May 29, 2009 (~5:06 pm start); Burst random (9Z-, 21Y-), 50% burst, ~90 lb-rms; 128 Hz sample rate, 0.03 125 Hz resolution, 20 averages, uniform window; Noticeable audible rattle internal—"thunder" sound; telehandler motion observed

SS5-10: May 29, 2009; Ambient data, 128 Hz sample rate, 0.03 125 Hz resolution, 40 averages; 9Z was disconnected from shaker/stinger rod removed

SS5-11: May 29, 2009 (~6:50 pm start); Sine sweep (21Y-), mode 2 characterization, 3.75 to 4.84 Hz; 10 lb-pk at 1 Hz/min; Run 2: 20 lb-pk at .5 Hz/min; Run 3: 20 lb-pk at .25 Hz/min, Range changed to 4.05 to 4.34 Hz for runs 4-6; Run 4: 20 lb-pk at .1 Hz/min; Run 5: 50 lb-pk at .1 Hz/min; Run 6: 100 lb-pk at .1 Hz/min

SS5-12: May 29, 2009 (~8:36 pm start); Sine sweep (21Y-), mode 4 characterization, 9.22 to 10.32 Hz; Run 1: 20 lb-pk at .2 Hz/min; Run 2: 100 lb-pk at .2 Hz/min

SS5-13: May 29, 2009 (~9:26 pm start); Sine sweep (9Z-), mode 3 characterization, 8.34 to 9.31 Hz; Run 1: 20 lb-pk at .2 Hz/min; Run 2: 100 lb-pk at .2 Hz/min

Post Test De-brief (~10 pm); based on quick look assessment data is satisfactory for calibration; ready to break configuration

Disconnected shakers and removed telehandlers; data acquisition system prepared for storage

Appendix E: Test Mode Shapes

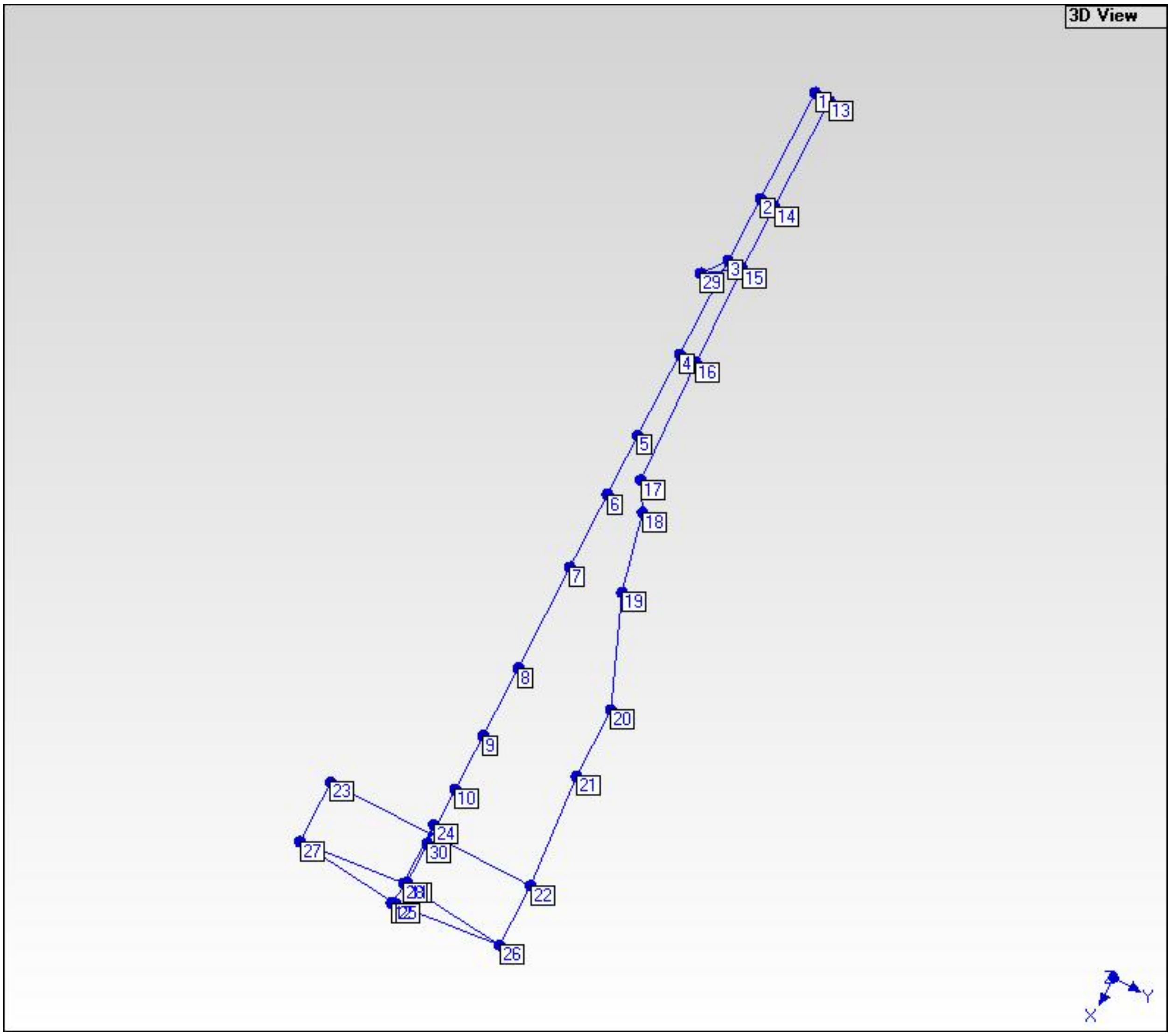

Figure E.1. Test geometry with measurement points labeled.

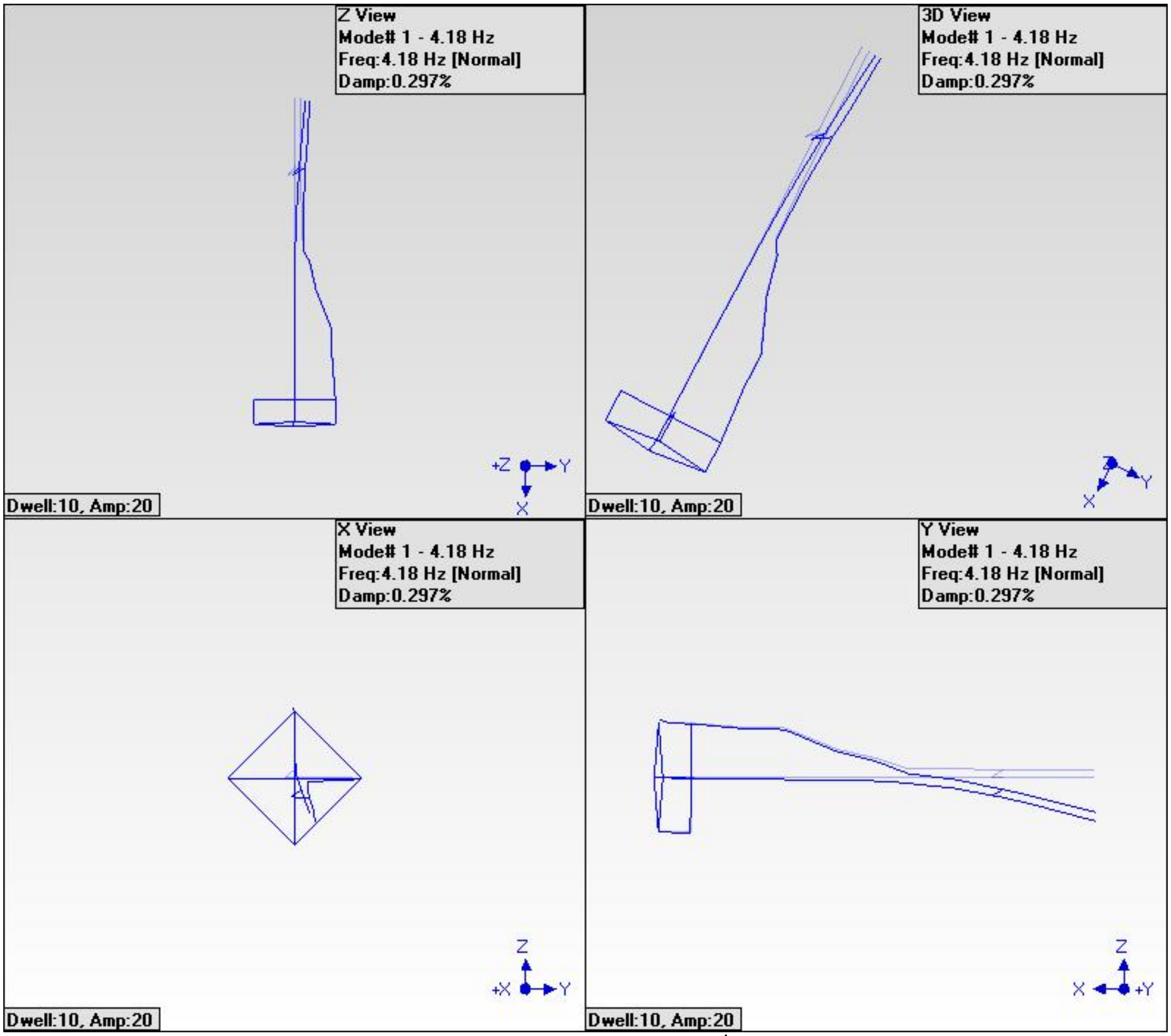

Figure E.2. Test mode 1; LAS 1st Bending.

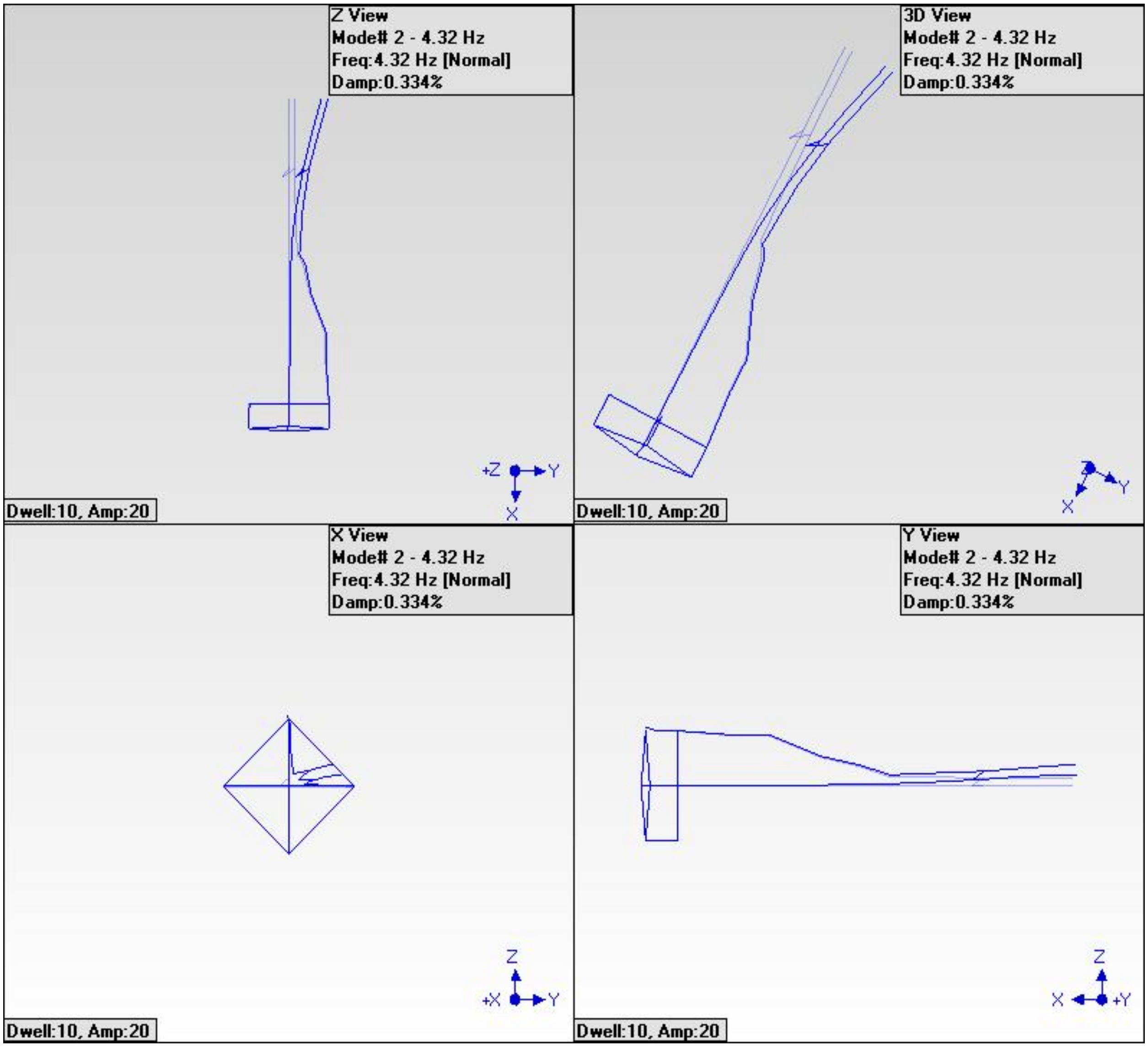

Figure E.3. Test mode 2; LAS 1st Bending.

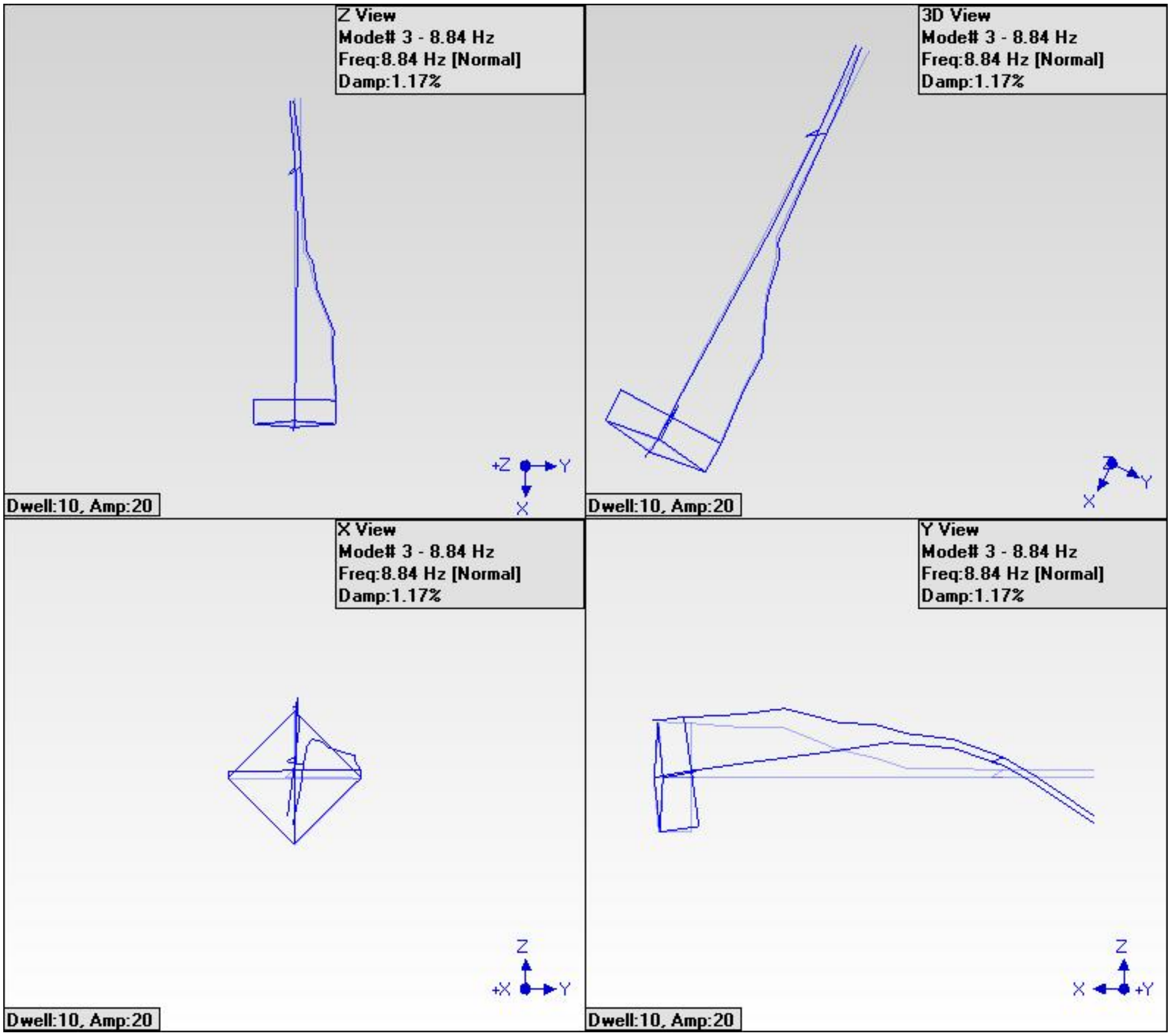

Figure E.4. Test mode 3; System Bending (X-Z Plane).

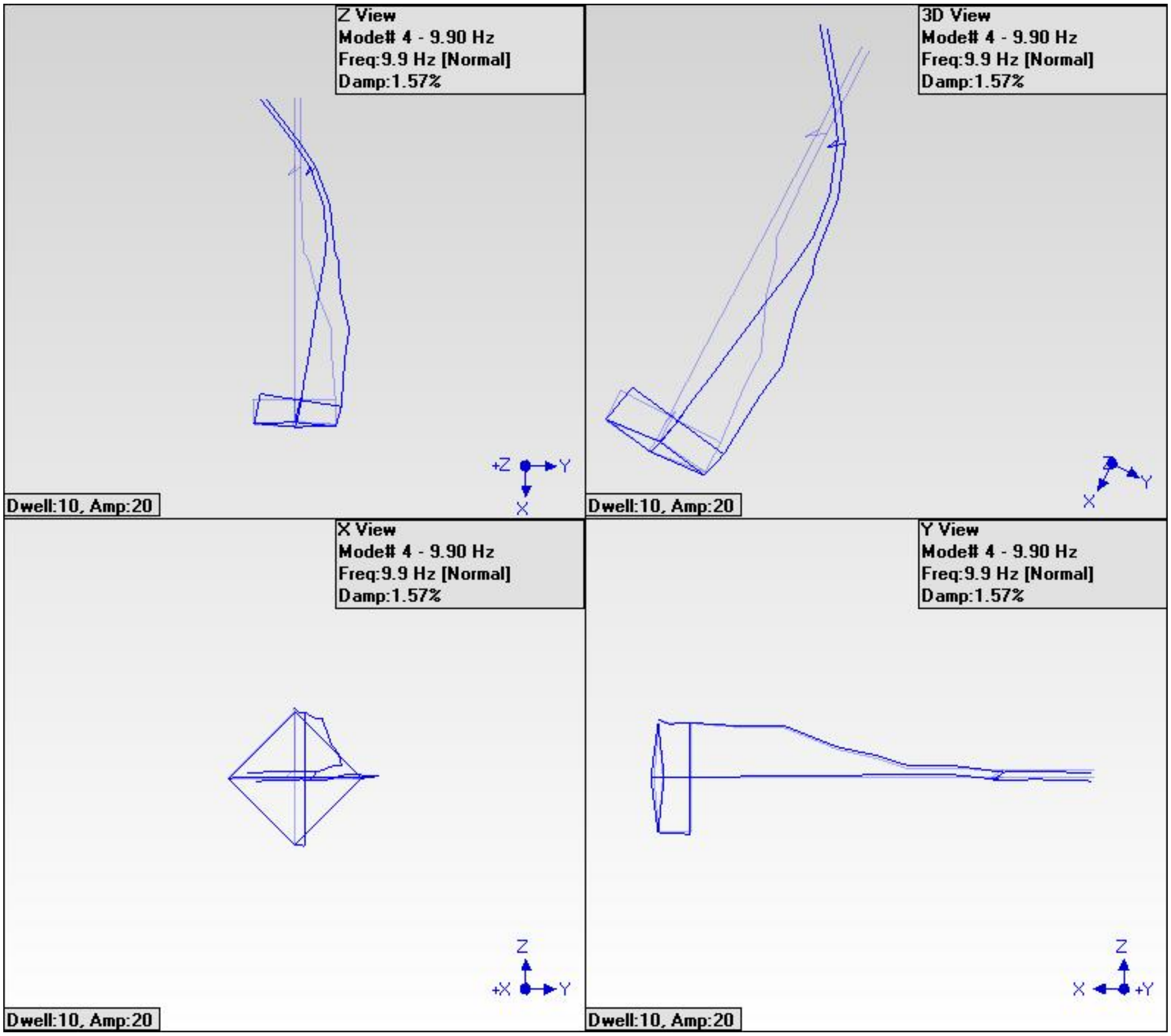

Figure E.5. Test mode 4; System Bending (X-Y Plane).

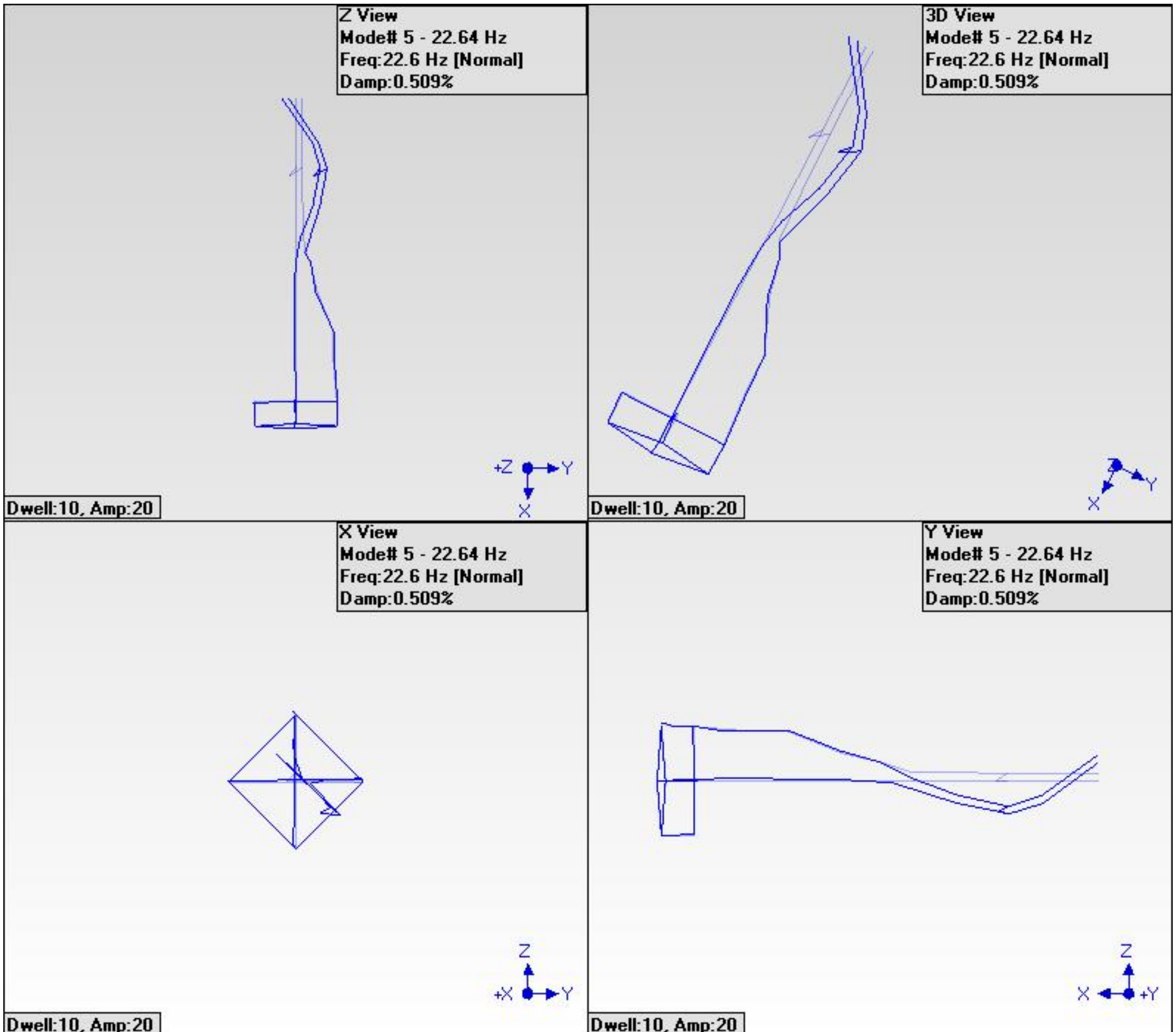

Figure E.6. Test mode 5; LAS 2nd Bending.

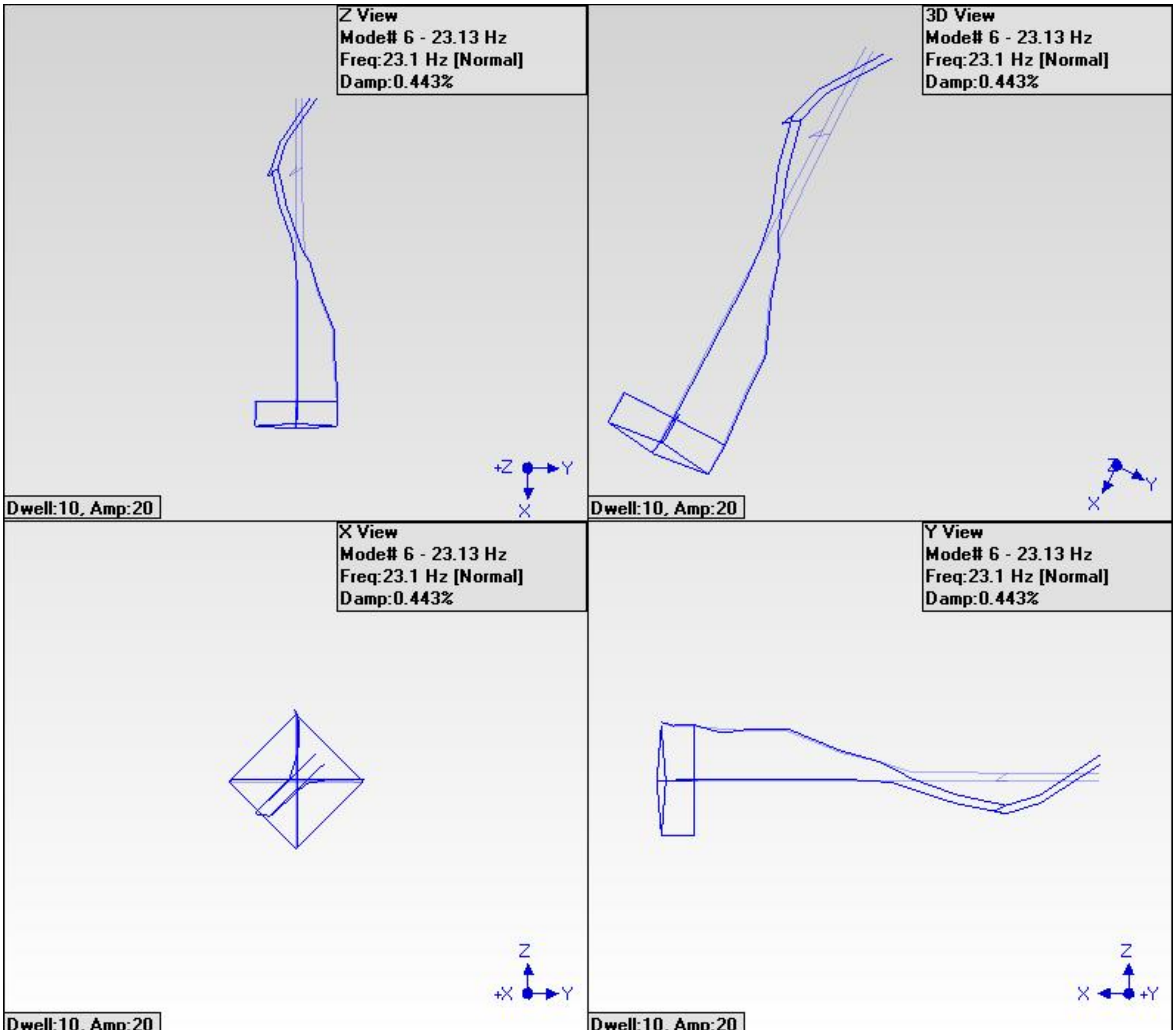

Figure E.7. Test mode 6; LAS 2nd Bending.

REPORT DOCUMENTATION PAGE	*Form Approved* *OMB No. 0704-0188*

1. REPORT DATE *(DD-MM-YYYY)*
01- 01 - 2010

2. REPORT TYPE
Technical Memorandum

3. DATES COVERED *(From - To)*

4. TITLE AND SUBTITLE
Ares I-X Flight Test Vehicle: Stack 5 Modal Test

5a. CONTRACT NUMBER

5b. GRANT NUMBER

5c. PROGRAM ELEMENT NUMBER

6. AUTHOR(S)
Buehrle, Ralph D.; Templeton, Justin D.; Reaves, Mercedes, C.; Horta, Lucas G.; Gaspar, James L.; Bartoletta, Paul A.; Parks, Russel A.; Lazor, Daniel R.

5d. PROJECT NUMBER

5e. TASK NUMBER

5f. WORK UNIT NUMBER
136905.10.10.20.20

7. PERFORMING ORGANIZATION NAME(S) AND ADDRESS(ES)
NASA Langley Research Center
Hampton, VA 23681-2199

8. PERFORMING ORGANIZATION REPORT NUMBER
L-19811

9. SPONSORING/MONITORING AGENCY NAME(S) AND ADDRESS(ES)
National Aeronautics and Space Administration
Washington, DC 20546-0001

10. SPONSOR/MONITOR'S ACRONYM(S)
NASA

11. SPONSOR/MONITOR'S REPORT NUMBER(S)
NASA/TM-2010-216183

12. DISTRIBUTION/AVAILABILITY STATEMENT
Unclassified - Unlimited
Subject Category 18
Availability: NASA CASI (443) 757-5802

13. SUPPLEMENTARY NOTES

14. ABSTRACT
Ares I-X was the first flight test vehicle used in the development of NASA's Ares I crew launch vehicle. The Ares I-X used a 4-segment reusable solid rocket booster from the Space Shuttle heritage with mass simulators for the 5th segment, upper stage, crew module and launch abort system. Three modal tests were defined to verify the dynamic finite element model of the Ares I-X flight test vehicle. Test configurations included two partial stacks and the full Ares I-X flight test vehicle on the Mobile Launcher Platform. This report focuses on the first modal test that was performed on the top section of the vehicle referred to as Stack 5, which consisted of the spacecraft adapter, service module, crew module and launch abort system simulators. This report describes the test requirements, constraints, pre-test analysis, test operations and data analysis for the Ares I-X Stack 5 modal test.

15. SUBJECT TERMS
Flight test vehicles; Modal parameters; Modal test; Verification

16. SECURITY CLASSIFICATION OF: a. REPORT	b. ABSTRACT	c. THIS PAGE	17. LIMITATION OF ABSTRACT	18. NUMBER OF PAGES	19a. NAME OF RESPONSIBLE PERSON
					STI Help Desk (email: help@sti.nasa.gov)
					19b. TELEPHONE NUMBER ***(Include area code)***
U	U	U	UU	62	(443) 757-5802

Standard Form 298 (Rev. 8-98)
Prescribed by ANSI Std. Z39.18